How can lattice QCD describe non-zero baryonic density ?

Ernst-Michael Ilgenfritz[1]

[1]Joint Institute for Nuclear Research, BLTP, Dubna, Russia

"Theory of hadronic matter under extremal conditions"
BLTP, Dubna, 10 and 17 August 2016

Outline

Outline

Outline

Outline

Outline

Outline

Outline

Outline

Outline

Outline

Outline

Outline

Outline

The phase diagram of QCD

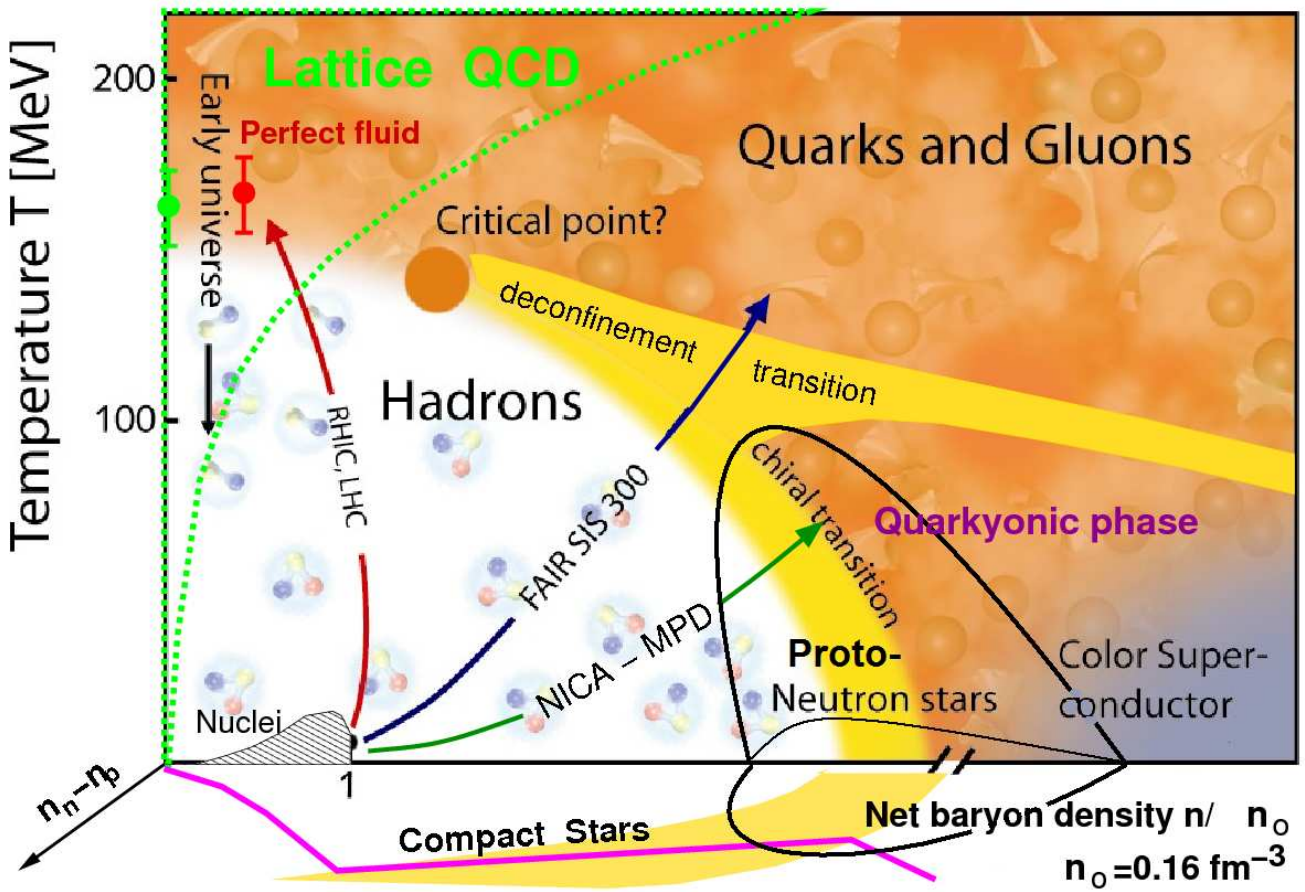

Figure: Sketch of the QCD phase diagram in the plane of temperature and net baryon density.

Is Lattice QCD capable to describe non-zero baryonic density ?

In short, the answer is "No, however we try ... and try to get estimates for the reliability of what we are doing"

"No", at least in the sense how LQCD has proven to be an ideal ("easy") machinery at zero baryonic density.

The region of large μ is more or less "terra incognita". It will be the target of heavy ion collisions at energies of NICA and FAIR. It seems natural that some activity should be directed to this field also in BLTP of JINR.

Finally, if only to describe the equilibrium states in the phase diagram, something like LQCD adapted to high baryonic density is highly needed.

Why Lattice QCD has been so successful at zero baryonic density ?

LQCD at $\mu = 0$ was/is a success story, because it ...

- allows straightforward simulations by importance sampling (possible due to choosing the Euclidean Lagrangian approach),
- allows a strict separation between positive definite measure and real-valued configuration space (the lattice field configurations),
- allows to inspect typical (real) lattice fields (in order to enquire possible mechanisms by indepth search),
- allows to calculate everything; one is not restricted to few particular observables (in some truncation they may be related through closed equations like SDE (Schwinger-Dyson equations) or similar continuum approaches like FRG).

Why Lattice QCD has been so successful at zero baryonic density ?

LQCD at $\mu = 0$ was/still is a success story, because ...

- a systematic improvement was possible towards the limit $a \to 0$ (continuum limit),
- a gradual improvement is possible towards the limit $V \to \infty$ (thermodynamical limit),
- these limits can be approached also for functions, for example for $U(r)$ (heavy quark potential), $G(p)$ (Greens functions), for vertices $\Gamma(p_1, p_2, p_3)$ etc. keeping the physical arguments (r or p_i) fixed.
- This made possible a productive interaction with continuum non-perturbative approaches (SDE and Functional Renormalization Group FRG).

What is so different in case of $\mu \neq 0$?

- Importance sampling is not possible anymore (due to the "sign problem", a complex weight problem).
- It is impossible to generate and store ensembles for different fixed densities.
- It is impossible to inspect configurations in order to figure out the microscopic "origin" of different physics (that we are alerted of by increasing "non-overlap").
- However, particular techniques are available to fight the sign problem for particular observables.
- Taylor expansion (in μ) of the measure at the zero-density limit is a multipurpose method, but has a finite convergence radius which is unknown *apriori* (different for different observables, say $\Delta p(\mu)$).
- Reweighting is meaningless : overlap problem, this becomes more and more severe beyond $\mu/T \approx 1$, a barrier that cannot be overcome !

The subject of this lecture

- Pointing out the origin of the trouble.
- Different ways to circumvent the problem, even though things are getting more and more intricate, much more expensive, less encouraging for the freshman, on the other hand more interesting !
- Few principally new methods for finite density $SU(3)$.

What I will **not discuss** here are

- possible side projects that usually may keep particle theorists busy in difficult times, particularly suitable for countries with a less-developed computing infrastructure.

Side projects hypothetically relevant for HIC

- Other gauge theories without sign problem:
  $SU(2)$, G_2, $SO(2N)$ .... when considered with μ_q

  V.V. Braguta (MIPT, ITEP, IHEP and FEFU), E.-M. I. (JINR), A.Yu. Kotov (MIPT and ITEP), A.V. Molochkov (FEFU), A.A. Nikolaev (ITEP and FEFU), "Study of the phase diagram of dense two-color QCD within lattice simulation", arXiv:1605.04090

This collaboration was inofficially founded as a four-sided HU Berlin–JINR–ITEP–Vladivostok collaboration by Mikhail Polikarpov († 2013), Michael Müller-Preussker († 2015) and myself at the "Confinement and Hadron Spectrum X" conference 2012 in Munich.

Side projects hypothetically relevant for HIC

- Other chemical potentials without sign problem: isospin chemical potential $\mu_{\rm iso}$, chiral chemical potential μ_5 (2 papers in 2015)

  V.V. Braguta (ITEP and FEFU), V.A. Goy (FEFU), E.-M. I. (JINR), A.Yu. Kotov (ITEP), A.V. Molochkov (FEFU), M. Müller-Preussker (HU Berlin), "Study of the phase diagram of SU(2) quantum chromodynamics with nonzero chirality", JETP Lett. 100 (2015) 547

  V.V. Braguta (IHEP and FEFU), V.A. Goy (FEFU), E.-M. I. (JINR), A.Yu. Kotov (ITEP), A.V. Molochkov (FEFU), M. Müller-Preussker, B. Petersson (HU Berlin), "Two-color QCD with non-zero chiral chemical potential", JHEP 1506 (2015) 094

Side projects hypothetically relevant for HIC

- Other chemical potentials without sign problem: isospin chemical potential $\mu_{\rm iso}$, chiral chemical potential μ_5 (2 papers in 2016)

  A.Yu. Kotov, V.V. Braguta (ITEP), V.A. Goy (FEFU), E.-M. I. (JINR), A.V. Molochkov (FEFU), M. Müller-Preussker, B. Petersson (HU Berlin), S.A. Skinderev (ITEP), "Lattice QCD with chiral chemical potential: from SU(2) to SU(3)", PoS LATTICE2015 (2016) 185

  V.V. Braguta (MIPT, ITEP, IHEP and FEFU), E.-M. I. (JINR), A. Yu. Kotov (MIPT and ITEP), B. Petersson (HU Berlin), S.A. Skinderev (ITEP), "Study of QCD phase diagram with non-zero chiral chemical potential", Phys. Rev. D93 (2016) 034509

Side projects hypothetically relevant for HIC

- characterizing topological excitations at imaginary chemical potential

  V.G. Bornyakov (ITEP, IHEP and FEFU), D.L. Boyda, V.A. Goy, A.V. Molochkov, A.A. Nikolaev (ITEP and FEFU), E.-M. I. (JINR), B.V. Martemyanov (ITEP, MEPhI and MIPT), A. Nakamura (Hiroshima U, RIKEN, RCNP Osaka and FEFU Vladivostok)
  "Dyons and the Roberge-Weiss transition in lattice QCD"
  (work in progress)
  Simulations underway with :
  $N_c = 3$ Iwasaki-improved gauge field action
  $N_f = 2$ clover-improved Wilson fermion flavors
  (similar to WHOT-QCD collaboration)

Outline

The partition function

$$Z(T,V,\mu) = \mathrm{Tr}\, e^{-(H-\mu N)/T} = e^{-F/T}.$$

The trace is understood in some basis of eigenstates. From the partition function, or free energy F, other thermodynamic quantities follow by differentiation with respect to T, μ, V, etc.

$$\langle N\rangle = T\frac{\partial}{\partial\mu}\ln Z, \qquad \langle n\rangle = \frac{1}{V}\langle N\rangle,$$

$$\langle \chi\rangle = \frac{1}{V}\left[\langle N^2\rangle - \langle N\rangle^2\right] = \frac{\partial\langle n\rangle}{\partial\mu}.$$

By studying the behaviour of these and other thermodynamic quantities while the external parameters like T and μ are changed, the phase structure can be scanned in $(T,\mu,H..)$ space. (also magnetic field H !)

Other thermodynamical functions derived from the partition function

From the partition function, all other thermodynamic equilibrium quantities also follow by taking appropriate derivatives: free energy, pressure, entropy, mean values of charges and the (internal) energy are obtained as

$$F = -T \ln Z \,, \qquad p = \frac{\partial (T \ln Z)}{\partial V} \,, \qquad S = \frac{\partial (T \ln Z)}{\partial T} \,,$$

$$\bar{N}_i = \frac{\partial (T \ln Z)}{\partial \mu_i} \,, \qquad E = -pV + TS + \mu_i \bar{N}_i \,.$$

When the partition function is known from any formalism (say, a Euclidean lattice calculation), all these relations remain valid.

Conserved charges

In QCD one may consider various conserved charges.
For simplicity, let's take two flavors, up and down, with chemical potentials μ_u, μ_d.
To obtain quark number, we choose the quark chemical potentials equal, $\mu_u = \mu_d = \mu_q$, such that

$$\langle n_q \rangle = \frac{T}{V} \frac{\partial}{\partial \mu_q} \ln Z = \langle n_u \rangle + \langle n_d \rangle .$$

Another possibility is to consider a nonzero isospin density. In that case, the chemical potentials are chosen opposite, $\mu_u = -\mu_d = \mu_{\rm iso}$, such that the isospin density equals

$$\langle n_{\rm iso} \rangle = \frac{T}{V} \frac{\partial}{\partial \mu_{\rm iso}} \ln Z = \langle n_u \rangle - \langle n_d \rangle .$$

Conserved charges

Finally, we might be interested in the electrical charge density and take the chemical potential proportional to the quarks' charge, $\mu_u = \frac{2}{3}\mu_Q, \mu_d = -\frac{1}{3}\mu_Q$, such that the electrical charge density is given by

$$\langle n_Q \rangle = \frac{T}{V}\frac{\partial}{\partial \mu_Q} \ln Z = \frac{2}{3}\langle n_u \rangle - \frac{1}{3}\langle n_d \rangle .$$

The partition function on the lattice

On the lattice, the QCD partition function is written not as Hilbert space trace over hadrons, but as an Euclidean path integral in terms of fundamental fields (quarks, gluons).

The advantage is not to **uncritically** anticipate a particular phase ! (as in the Hadron Resonance Gas model ! inspired by Hagedorn's Statistical Bootstrap)

It is formulated in terms of the links $U_{x\nu} = e^{iaA_{x\nu}}$, with $A_{x\nu}$ the vector potential with a as the lattice spacing. The inverse temperature is given by the extent in the temporal direction, $1/T = aN_\tau$, with N_τ being the number of time slices.

$$Z = \int DUD\bar{\psi}D\psi\, e^{-S} = \int DU\, e^{-S_{\rm YM}} \det M(U,\mu).$$

The lattice action

U denotes the gauge links and $\psi, \bar{\psi}$ the quark fields.

The QCD action has the following schematic form

$$S = S_{\mathrm{YM}} + S_{\mathrm{F}}$$

with

$$S_{\mathrm{F}} = \int d^4x\, \bar{\psi} M(U,\mu) \psi .$$

S_{YM} is the Yang-Mills action, consisting of closed loops formed out of links $U_{x\mu}$ (e.g. plaquettes, see later). $M(U,\mu)$ denotes the fermion matrix of a bilinear form, depending on all links $U_{x\mu}$ and the chemical potential(s). Integrating over the quark fields yields the above form, a result, which contains the determinant $\det M$.

Simulation by importance sampling of gauge link configurations

Now, in numerical simulations the integrand,

$$\rho(U) \sim e^{-S_{\rm YM}} \det M(U,\mu),$$

would be a (usually real and positive) probability weight such that configurations of gauge links can be generated, relying on importance sampling. Thus, some version of importance sampling (Hybrid Monte Carlo etc.) can be used.

At non-zero baryonic chemical potential, however, the fermion determinant turns out to be complex,

$$[\det M(U,\mu)]^* = \det M(U,-\mu^*) \in \mathbb{C}.(*)$$

As a result, the weight $\rho(U)$ in total is complex and standard numerical algorithms based on importance sampling are not applicable.

The emergence of the "sign problem"

This is sometimes referred to as the "sign problem", even though "complex-phase problem" would be more appropriate.

In particle physics, it appears not only in QCD.

It appears also, if one goes to Minkowski space (formulating real-time quantum dynamics).

It appears in other branches of theoretical physics as well (for example, condensed matter and polymer physics).

Nowadays, it is recognized as one **central problem in mathematical and computational physics** (Topical Workshops, Topical Task Force Programs ...).

It is closely related to "Resurgence Field Theory" ..., which unifies perturbative and non-perturbative physics.

Chemical potential for fermion fields in the continuum

The presence of the complex-phase problem is NOT restricted to (induced exclusively by) fermions !
Discussing fermions first, here is the Euclidean action for non-interacting fermions :

$$S = \int_0^{1/T} d\tau \int d^3x\, \bar{\psi}\left(\gamma_\nu \partial_\nu + m\right)\psi.$$

Due to the global symmetry

$$\psi \to e^{i\alpha}\psi, \qquad \bar{\psi} \to \bar{\psi} e^{-i\alpha},$$

fermion number is a conserved charge,

$$N = \int d^3x\, \bar{\psi}\gamma_4\psi = \int d^3x\, \psi^\dagger\psi \qquad \Rightarrow \qquad \partial_\tau N = 0.$$

Introducing chemical potential of fermion fields into the action

To obtain the grand canonical partition function in the Euclidean path integral formulation, one adds the following term to the action,

$$\frac{\mu N}{T} = \frac{\mu}{T}\int d^3x\,\bar{\psi}\gamma_4\psi = \int_0^{1/T} d\tau \int d^3x\,\mu\bar{\psi}\gamma_4\psi,$$

$$N = \int d^3x\,\bar{\psi}\gamma_4\psi = \int d^3x\,\psi^\dagger\psi \qquad \Rightarrow \qquad \partial_\tau N = 0.$$

which reads, after inclusion of an Abelian gauge field A_ν

$$\begin{aligned} S &= \int_0^{1/T} d\tau \int d^3x\,\bar{\psi}\left[\gamma_\nu(\partial_\nu + iA_\nu) + \mu\gamma_4 + m\right]\psi \\ &= \int d^4x\,\bar{\psi}\,M(A,\mu)\,\psi. \end{aligned}$$

A few observations:

- μ appears in the same way as iA_4, i.e. as the imaginary part of the four-component of an abelian vector field. This will be important when chemical potential is introduced in the lattice formulation.
- Generically, the action is complex. This can be seen by the absence of "γ_5 hermiticity".
  At $\mu = 0$ it is easy to see that

$$(\gamma_5 M)^\dagger = \gamma_5 M, \qquad M^\dagger = \gamma_5 M \gamma_5,$$

  leading to

$$\det M^\dagger = \det(\gamma_5 M \gamma_5) = \det M = (\det M)^*,$$

  i.e. the determinant is real. Otherwise, for $\mu \neq 0$

$$M^\dagger(\mu) = \gamma_5 M(-\mu^*)\gamma_5,$$

  resulting in Eq. (*), therefore a complex determinant.

Few more observations:

- When the chemical potential is purely imaginary, the determinant is real again. This has been exploited extensively and will be discussed later.
- For Abelian gauge theories, the chemical potential can be removed by a simple gauge transformation of A_4 (choose μ imaginary and use analyticity). This is no longer true in Non-Abelian $SU(N)$ theories or for theories with more than one chemical potential.
- The sign problem is not specific for fermions. In particular, it is not due to the Grassmann nature of fermionic fields.
- The sign problem arises from the complexity of the determinant (in case of fermions) or complexity of the action in general, in any path integral weight.

Chemical potential for bosonic fields in the continuum

Consider a complex scalar field with a global symmetry $\phi \to e^{i\alpha}\phi$. The action is

$$S = \int d^4x \left(|\partial_\nu \phi|^2 + m^2 |\phi|^2 + \lambda |\phi|^4 \right),$$

and the conserved charge is written

$$N = \int d^3x \, i \left[\phi^* \partial_4 \phi - (\partial_4 \phi^*) \phi \right].$$

The partition function in its Hilbert space form is again

$$Z = \mathrm{Tr}\, e^{-(H-\mu N)/T}.$$

Before one expresses this in path integral form, the Hamiltonian and the conserved charge (densities) must be expressed in terms of the canonical momenta $\pi_1 = \partial_4 \phi_1, \pi_2 = \partial_4 \phi_2$, where $\phi = (\phi_1 + i\phi_2)/\sqrt{2}$.

Chemical potential for bosonic fields in path integral form

For example, the charge now takes the form

$$N = \int d^3x \, (\phi_2 \pi_1 - \phi_1 \pi_2) \, .$$

The partition function reads in the Euclidean phase space path integral form

$$\begin{aligned} Z &= \mathrm{Tr}\, e^{-(H-\mu N)/T} \\ &= \int D\phi_1 D\phi_2 \int D\pi_1 D\pi_2 \\ &\quad \times \exp \int d^4x \left[i\pi_1 \partial_4 \phi_1 + i\pi_2 \partial_4 \phi_2 - \mathcal{H} + \mu(\phi_2 \pi_1 - \phi_1 \pi_2) \right] \end{aligned}$$

After integrating out the momenta (done as usual), one finds the Euclidean action in the path integral (over ϕ alone is now integrated, no integration over π is left).

Chemical potential for bosonic fields in the Euclidean action

$$S = \int d^4x \left[(\partial_4 + \mu)\phi^*(\partial_4 - \mu)\phi + |\partial_i \phi|^2 + m^2|\phi|^2 + \lambda|\phi|^4 \right].$$

$$S =$$

$$\int d^4x \left[|\partial_\nu \phi|^2 + (m^2 - \mu^2)|\phi|^2 + \mu(\phi^* \partial_4 \phi - \partial_4 \phi^* \phi) + \lambda|\phi|^4 \right]$$

- The chemical potential appears again as an imaginary vector potential.
- The term linear in μ is purely imaginary, resulting in a complex action $S^*(\mu) = S(-\mu^*)$.
- The term quadratic in μ arose from integrating out the momenta. This is absent in fermionic theories.

The Silver Blaze problem: a miraculous μ-independence for low T at $\mu < \mu_{\rm onset}$?

Consider a particle with mass m and a conserved charge at low temperature: as usual, μ is the change in free energy **(work)** when a particle carrying the conserved charge is added, i.e. the energy reservoir for adding one particle. Hence it is plausible that

- if $\mu < m$: not enough energy available to create a new particle $\Rightarrow$ no change in the groundstate;
- if $\mu > m$: plenty of energy available $\Rightarrow$ now the groundstate acquires a nonzero density of particles.

Hence it follows from simple statistical mechanics that at zero temperature the density becomes nonzero (a.k.a. "onset") only for $\mu > \mu_{\rm onset} \equiv m$. This will be demonstrated for free fermions.

The Essence of the Silver Blaze problem

In general, the term "Silver Blaze" denotes a miraculous (almost-) independence of μ at low enough T throughout the interval $0 < \mu < \mu_{\rm onset}$,
where $\mu_{\rm onset} = \mathcal{O}(\text{some characteristic mass of the theory})$.

This (almost-) independence has its origin in cancellations related to the sign problem.

These cancellations are eventually absent in a **not adequately substituted theory** (e.g. the "phase quenched theory"). This one is simply misleading (no approximation at all!) because it actually represents other, "wrong" physics !

The complex phase problem is not a minor defect !
It is necessary to reproduce the correct physics.

There would be no free energy difference between quark and antiquark without $\mathrm{Im}(\det M) \neq 0$! (Ph. de Forcrand)

$$\langle \mathrm{Tr\ Polyakov}\ \rangle = \exp(-\frac{1}{T}F_q)$$

$$= \int\ [\mathrm{Re(P)} \times \mathrm{Re(det\,M)} - \mathrm{Im(P)} \times \mathrm{Im(det\,M)}]\, e^{-S_{YM}}\, DU$$

$$\langle \mathrm{Tr\ Polyakov}^{+}\rangle = \exp(-\frac{1}{T}F_{\bar{q}})$$

$$= \int\ [\mathrm{Re(P)} \times \mathrm{Re(det\,M)} + \mathrm{Im(P)} \times \mathrm{Im(det\,M)}]\, e^{-S_{YM}}\, DU$$

For $SU(2), N_f = 2$, the square of the determinant remains real positive even when $\mu \neq 0$. But the μ_q can be turned into μ_{iso} by a redefinition of the quark fields.

The Silver Blaze problem is not unfamiliar from standard thermodynamics with mass m

The standard expression for the logarithm of the partition function for a free relativistic fermion gas with mass m is

$$\ln Z = 2V \int \frac{d^3p}{(2\pi)^3} \left[\beta\omega_{\mathbf{p}} + \ln\left(1 + e^{-\beta(\omega_{\mathbf{p}} - \mu)}\right) + \ln\left(1 + e^{-\beta(\omega_{\mathbf{p}} + \mu)}\right) \right],$$

where $\omega_{\mathbf{p}} = \sqrt{\mathbf{p}^2 + m^2}$ and $\beta = 1/T$.
2 is the spin factor, the first term is the zero-point energy and the other terms represent particles and anti-particles at nonzero temperature and chemical potential.
The fermion minus antifermion density is

$$\langle n \rangle = \frac{T}{V}\frac{\partial \ln Z}{\partial \mu} = 2 \int \frac{d^3p}{(2\pi)^3} \left[\frac{1}{e^{\beta(\omega_{\mathbf{p}} - \mu)} + 1} - \frac{1}{e^{\beta(\omega_{\mathbf{p}} + \mu)} + 1} \right].$$

The two cases, below and above onset m

We consider the low-temperature limit, $T \to 0$.
We distinguish two cases (separated by m):

- $\mu < m$: the '1' in the denominator of the Fermi-Dirac distribution can be ignored and

$$\langle n \rangle \sim 2 \int \frac{d^3p}{(2\pi)^3} \left[e^{-\beta(\omega_{\mathbf{p}} - \mu)} - e^{-\beta(\omega_{\mathbf{p}} + \mu)} \right] \to 0.$$

  Particles and antiparticles are only thermally excited and therefore Boltzmann suppressed.

- $\mu > m$: in this case μ can be larger than $\omega_{\mathbf{p}}$, the Fermi-Dirac distribution becomes a step function at $T = 0$, further rising like $\sim \mu^3$:

$$\langle n \rangle \sim 2 \int \frac{d^3p}{(2\pi)^3} \Theta(\mu - \omega_{\mathbf{p}}) = \frac{\left(\mu^2 - m^2\right)^{3/2}}{3\pi^2} \Theta(\mu - m).$$

  As expected, nonzero density for $\mu > m$ (i.e. "onset").

Outline

Introducing a chemical potential for lattice fermions

The naive way, adding $\mu\bar{\psi}\gamma_4\psi$ to the action, leads to μ-dependent ultraviolet divergences like what appears in the energy density, $\epsilon(\mu) - \epsilon(0) \sim \left(\frac{\mu}{a}\right)^2$.

Instead, we better follow the observations made in the continuum :

- the chemical potential couples to the 4-th component of the corresponding conserved point-split current;
- it appears as the imaginary part of the fourth component of an Abelian vector field.

The terms in the action from which the conserved lattice current follows, the so-called hopping terms, are

$$S \sim \bar{\psi}_x U_{x\nu}\gamma_\nu\psi_{x+\nu} - \bar{\psi}_{x+\nu} U^\dagger_{x\nu}\gamma_\nu\psi_x,$$

for all directions $\nu = 1, 2, 3, 4$.

Introducing a chemical potential for lattice fermions

The exactly conserved (point-split) current reads then

$$j_\nu \sim \bar{\psi}_x U_{x\nu} \gamma_\nu \psi_{x+\nu} + \bar{\psi}_{x+\nu} U^\dagger_{x\nu} \gamma_\nu \psi_x .$$

Chemical potential is now introduced as an imaginary Abelian vector field in the 4-direction, i.e. multiplying the (non-Abelian) links by Abelian factors exp $(\pm a\mu)$

$$\text{forward hopping:} \quad U_{x4} = e^{iA_{4x}} \quad \Rightarrow \quad e^{a\mu} U_{x4},$$
$$\text{backward hopping:} \quad U^\dagger_{x4} = e^{-iA_{4x}} \quad \Rightarrow \quad e^{-a\mu} U^\dagger_{x4}.$$

Features of this construction :

- the correct (naive) continuum limit is preserved,
- μ couples to the exactly conserved charge, even at finite lattice spacing a,
- no additional ultraviolet divergences are generated.

Consequence of chemical potential of lattice fermions: forward and backward hopping get different weight in the determinant

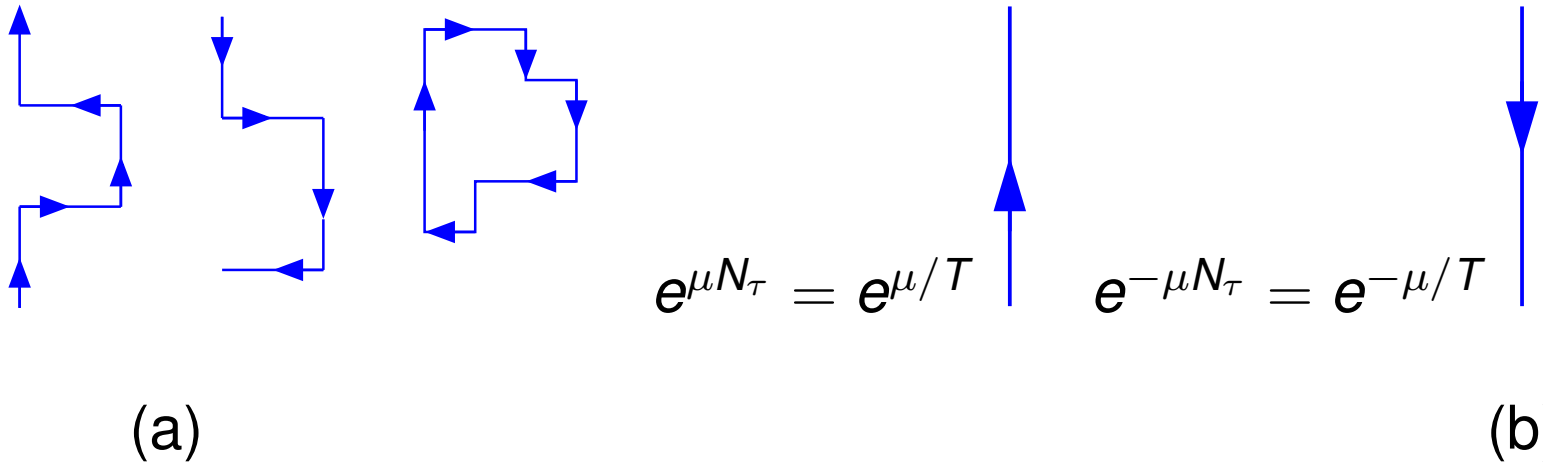

Figure: (a) Forward (backward) hopping is (dis)favoured by $e^{\mu n_\tau}$ ($e^{-\mu n_\tau}$), while closed loops are μ-independent. (b) Loops wrapping around the temporal direction contribute $e^{\pm \mu/T}$. This interpretation is useful for the hopping parameter expansion or any decomposition (say, by reduction formulae) of the fermion determinant ! It suggests that imaginary μ is equivalent to phase-rotated boundary conditions for wrapping in 4-direction.

Consequence of chemical potential of lattice bosons : a closed solution for $\lambda = 0$

Consider a self-interacting complex scalar field in the presence of a chemical potential μ, with the continuum action $S =$

$$\int d^4x \left[|\partial_\nu \phi|^2 + (m^2 - \mu^2)|\phi|^2 + \mu(\phi^* \partial_4 \phi - \partial_4 \phi^* \phi) + \lambda |\phi|^4 \right]$$

The Euclidean action is complex and satisfies $S^*(\mu) = S(-\mu^*)$. Take $m^2 > 0$, such that at vanishing μ and small μ the theory is in the symmetric phase.
The lattice action (lattice spacing $a_{\rm lat}$ put equal 1) is

$$S = \sum_x \left[\left(2d + m^2\right) \phi_x^* \phi_x + \lambda \left(\phi_x^* \phi_x\right)^2 \right.$$

$$\left. - \sum_{\nu=1}^{4} \left(\phi_x^* e^{-\mu \delta_{\nu,4}} \phi_{x+\hat{\nu}} + \phi_{x+\hat{\nu}}^* e^{\mu \delta_{\nu,4}} \phi_x \right) \right].$$

Solving the lattice boson problem with non-zero chemical potential

The complex field is written in terms of two real fields ϕ_a $(a = 1, 2)$ as $\phi = \frac{1}{\sqrt{2}}(\phi_1 + i\phi_2)$. The lattice action reads

$$S = \sum_x \left[\frac{1}{2}\left(2d + m^2\right)\phi_{a,x}^2 + \frac{\lambda}{4}\left(\phi_{a,x}^2\right)^2 - \sum_{i=1}^{3} \phi_{a,x}\phi_{a,x+\hat{i}} \right.$$
$$\left. - \cosh\mu\, \phi_{a,x}\phi_{a,x+\hat{4}} + i \sinh\mu\, \varepsilon_{ab}\phi_{a,x}\phi_{b,x+\hat{4}} \right].$$

ε_{ab} = antisymmetric tensor with $\epsilon_{12} = 1$
(a "hopping term" interchanging $1 \longleftrightarrow 2$).

The $\sinh\mu$ term is the imaginary part of the action.
From now on the self-interaction is ignored and we take $\lambda = 0$. The action is now reduced to bilinear form (which renders the problem directly solvable).

Consequence of chemical potential of lattice bosons: Gaussian path integral, has a closed solution

In momentum space the action reads

$$S = \sum_p \frac{1}{2}\phi_{a,-p}\left(\delta_{ab}A_p - \varepsilon_{ab}B_p\right)\phi_{b,p} = \sum_p \frac{1}{2}\phi_{a,-p}M_{ab,p}\phi_{b,p},$$

where

$$M_p = \begin{pmatrix} A_p & -B_p \\ B_p & A_p \end{pmatrix},$$

and

$$\begin{aligned} A_p &= m^2 + 4\sum_{i=1}^{3}\sin^2\frac{p_i}{2} + 2\left(1 - \cosh\mu\cos p_4\right), \\ B_p &= 2\sinh\mu\sin p_4. \end{aligned}$$

Consequence of chemical potential of lattice bosons: Gaussian path integral, closed solution

The propagator corresponding to the action is

$$G_{ab,p} = \frac{\delta_{ab} A_p + \varepsilon_{ab} B_p}{A_p^2 + B_p^2}.$$

The dispersion relation that follows from the poles of the propagator, taking $p_4 = iE_{\mathbf{p}}$, reads

$$\cosh E_{\mathbf{p}}(\mu) = \cosh \mu \left(1 + \tfrac{1}{2}\hat{\omega}_{\mathbf{p}}^2\right) \pm \sinh \mu \sqrt{1 + \frac{1}{4}\hat{\omega}_{\mathbf{p}}^2},$$

where

$$\hat{\omega}_{\mathbf{p}}^2 = m^2 + 4 \sum_i \sin^2 \frac{p_i}{2}.$$

This can be written (thanks to the addition theorem for the hyperbolic cosh) as

$$\cosh E_{\mathbf{p}}(\mu) = \cosh\left[E_{\mathbf{p}}(0) \pm \mu\right],$$

Comparison of the spectrum between full and phase-quenched theory

Thus, the (positive energy) solutions in the theory are

$$E_{\mathbf{p}}(\mu) = E_{\mathbf{p}}(\mu = 0) \pm \mu.$$

The critical μ value for onset is $\mu_c = E_{\mathbf{0}}(0)$, so that one mode becomes exactly massless at the transition μ_c (Goldstone boson).
The phase-quenched theory, in contrast, corresponds to putting $\sinh \mu = B_p = 0$ (removal of the imaginary part of action). The dispersion relation in the phase-quenched theory is then completely different:

$$\cosh E_{\mathbf{p}}(\mu) = \frac{1}{\cosh \mu} \left(1 + \tfrac{1}{2}\hat{\omega}^2_{\mathbf{p}}\right),$$

corresponding to $E^2_{\mathbf{p}}(\mu) = m^2 - \mu^2 + \mathbf{p}^2 = E^2_{\mathbf{p}}(\mu = 0) - \mu^2$ in the continuum limit.

Exercises I

- Compare the spectrum of the full and the phase-quenched theory, when $\mu < \mu_c$.
- At larger μ, it is necessary to include the self-interaction λ to stabilize the theory.
- Based on what you know about symmetry breaking, sketch the spectrum in the full and the phase-quenched theory also for larger μ.

Are the thermodynamic quantities independent of μ at vanishing temperature ?

Although the spectrum depends on μ, thermodynamic quantities do not. Up to an irrelevant constant, the logarithm of the partition function is

$$\ln Z = -\frac{1}{2}\sum_p \ln\det M = -\frac{1}{2}\sum_p \ln(A_p^2 + B_p^2),$$

and some observables are given by

$$\langle|\phi|^2\rangle = -\frac{1}{\Omega}\frac{\partial \ln Z}{\partial m^2} = \frac{1}{\Omega}\sum_p \frac{A_p}{A_p^2 + B_p^2},$$

and

$$\langle n\rangle = \frac{1}{\Omega}\frac{\partial \ln Z}{\partial \mu} = -\frac{1}{\Omega}\sum_p \frac{A_p A_p' + B_p B_p'}{A_p^2 + B_p^2},$$

where $\Omega = N_\sigma^3 N_\tau$ and $A_p' = \partial A_p/\partial\mu$, $B_p' = \partial B_p/\partial\mu$.

Exercises II

Difference compared to the phase-quenched theory ?

- Evaluate the sums (e.g. numerically) to demonstrate that thermodynamic quantities are independent of μ in the thermodynamic limit at vanishing temperature, but this holds only in the full theory !

These exercises are based on G. Aarts, JHEP 0905 (2009) 052, arXiv:0902.4686

Outline

How to deal with the complex weight in practical simulations ?

A prompt (but naive !) answer would be:

- simplify the weight for sampling, just neglecting the phase which usually is preventing the sampling;
- account for the phase factor later by reweighting (in the moment when calculating observables).

Let us consider again the partition function

$$Z = \int DUD\bar{\psi}D\psi\, e^{-S} = \int DU\, e^{-S_B} \det M, \qquad (1)$$

with a complex determinant,

$$\det M = |\det M|\; e^{i\varphi}. \qquad (2)$$

An seemingly straightforward solution to the complex-phase problem is to "absorb" the phase factor into the observable, just as a reweighting factor.

Phase quenching

$$\begin{aligned}\langle O\rangle_{\text{full}} &= \frac{\int DU\, e^{-S_B} \det M\, O}{\int DU\, e^{-S_B} \det M} \\ &= \frac{\int DU\, e^{-S_B} |\det M|\, e^{i\varphi} O}{\int DU\, e^{-S_B} |\det M|\, e^{i\varphi}} \\ &= \frac{\langle e^{i\varphi} O\rangle_{\text{pq}}}{\langle e^{i\varphi}\rangle_{\text{pq}}}.\end{aligned}$$

$\langle\cdot\rangle_{\text{full}}$ denotes expectation values taken with respect to the original, complex weight $\rho(U) \propto \det M$,

$\langle\cdot\rangle_{\text{pq}}$ denotes expectation values with respect to the "phase-quenched" weight, i.e. using $\rho(U) \propto |\det M|$.

Why is phase quenching useless closer to the thermodynamical limit ?

Look at the "average phase factor" $\langle e^{i\varphi} \rangle_{\rm pq}$.
This has the form of a ratio of two partition functions :

$$\langle e^{i\varphi} \rangle_{\rm pq} = \frac{\int DU\, e^{-S_B} |\det M|\, e^{i\varphi}}{\int DU\, e^{-S_B} |\det M|} = \frac{Z_{\rm full}}{Z_{\rm pq}} = e^{-\Omega \Delta f},$$

where we have expressed the partition functions in terms of the free energy densities,

$$Z \equiv Z_{\rm full} = e^{-F/T} = e^{-\Omega f_{\rm full}}, \qquad Z_{\rm pq} = e^{-F_{\rm pq}/T} = e^{-\Omega f_{\rm pq}},$$

with Ω the spacetime volume ($\Omega = V/T$ in physical units or $N_\tau N_s^3$ in lattice units), and

$$\Delta f = f_{\rm full} - f_{\rm pq} > 0$$

is the difference of the free energy densities.
Obviously, the following inequality holds: $Z_{\rm full} \leq Z_{\rm pq}$.

Overlap problem

The expectation value, that one is seeking for,

$$\langle O \rangle_{\rm full} = \frac{\langle e^{i\varphi} O \rangle_{\rm pq}}{\langle e^{i\varphi} \rangle_{\rm pq}}$$

is of exponentially undefined type "0/0" in the limit $V \to \infty$.

One says: "The sign problem is exponentially hard."

Physics of the two ensembles differs in an essential way: if they share (only few) configurations at all, these are possessing strongly different weight in the respective ensembles.

What different physics corresponds to the phase-quenched ensemble compared to the fixed-baryon-density ensemble ?

Overlap problem = missing overlap between ensembles

Consider two mass-degenerate flavors. $|\det M|$ not easy !

fixed quark density ensemble $\quad \rho(U) \propto [\det\ M(\mu)]^2$

whereas the

phase quenched ensemble $\quad \rho(U) \propto |\det\ M(\mu)|^2$

$$\propto \det\ M^\dagger(\mu)\ \det\ M(\mu)$$

$$\propto \det\ M(-\mu)\ \det\ M(\mu),$$

is actually corresponding to an isospin chemical potential with a value $\mu_{\rm iso} = \mu$ coinciding with μ.
Difference of phase structure (in μ_q vs. $\mu_{\rm iso} = \mu_u = -\mu_d$ is easy to understand physically (but difficult to understand in terms of gauge configurations !).
Undiscovered topological features ?
"Disoriented" condensates ?

A severe sign problem exists due to pion condensation

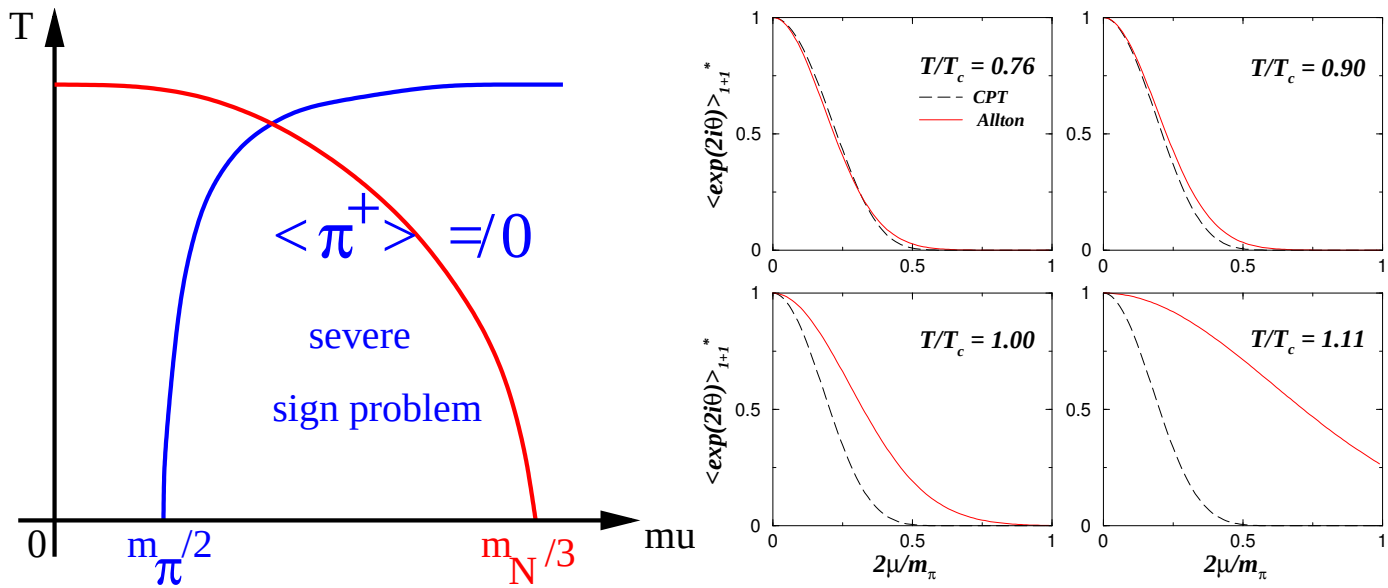

Figure: *Left*: Sketch of the QCD pseudo-critical line $T_c(\mu)$ (in red), starting from $\sim m_N/3$ at $T = 0$, superimposed with the phase transition line (in blue) of the phase-quenched theory (*alias* isospin chemical potential), starting pion condensation from $m_\pi/2$ at $T = 0$. *Right*: Comparison of values of the "average phase factor" $\langle \exp(2i\theta) \rangle$, measured in lattice simulations and predicted by one-loop χPT (Splittorff 2007). Good agreement with χPT persists up to $T/T_c \sim 0.90$.

Average phase factor in the phase-quenched theory at $T = 0$

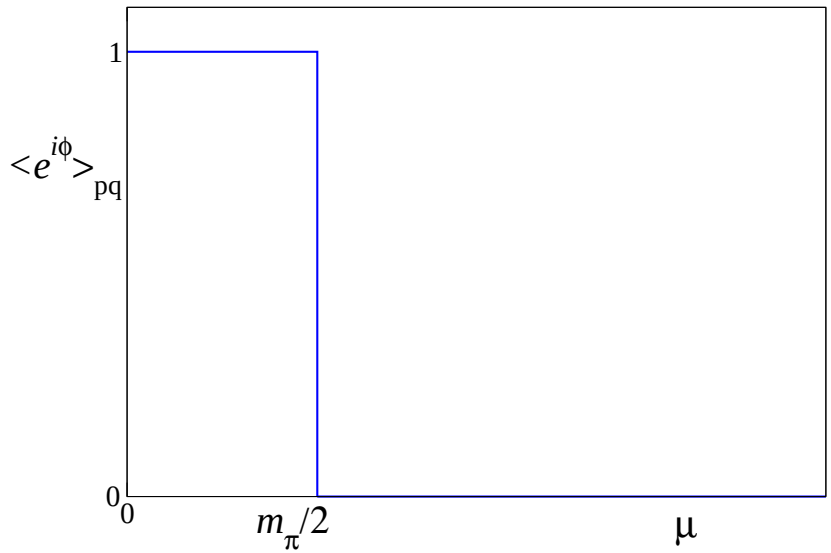

Figure: Average phase factor in the thermodynamic limit $V \to \infty$ in the phase-quenched theory at $T = 0$. In other words, throughout the interval $0 < \mu < m_\pi/2$ phase quenching is not misleading at $T = 0$! But no interesting physics is happening there in both theories ! In the interval $0 < \mu < m_N/3$, however, strong cancellations are required to cancel the unwanted μ-dependence from the full theory.

Silver blaze problem from the Dirac operator's eigenvalue point of view

Consider the Dirac operator as

$$M = D + m \qquad \text{with} \qquad D = \not{D} + \mu\gamma_4 .$$

The partition function is written as

$$Z = \int DU \, \det(D+m) e^{-S_{\rm YM}} = \langle\langle \det(D+m) \rangle\rangle_{\rm YM},$$

where the subscript YM indicates the average over the gluonic field only. (The brackets $\langle\langle\cdot\rangle\rangle_{\rm YM}$ are not normalized like expectation values !)
The determinant is the product of the eigenvalues,

$$\det(D+m) = \prod_k (\lambda_k + m) \qquad\qquad D\psi_k = \lambda_k \psi_k .$$

Note that since D is not γ_5 hermitian at nonzero μ, the eigenvalues are complex (a cloud in complex plane).

Silver blaze problem for the chiral condensate

Look at the chiral condensate, which is expressed as

$$\langle\bar\psi\psi\rangle = \frac{1}{\Omega}\frac{\partial \ln Z}{\partial m} = \frac{1}{Z}\left\langle\left\langle \frac{1}{\Omega}\sum_k \frac{1}{\lambda_k + m}\prod_j(\lambda_j+m)\right\rangle\right\rangle_{\rm YM},$$

since the derivative with respect to m removes every factor $\lambda_k + m$ from the determinant once. This can be written in terms of the density of eigenvalues, defined as

$$\rho(z;\mu) = \frac{1}{Z}\int DU\,\det(D+m)e^{-S_{\rm YM}}\frac{1}{\Omega}\sum_k \delta^2(z-\lambda_k)$$

$$= \frac{1}{Z}\left\langle\left\langle \det(D+m)\frac{1}{\Omega}\sum_k \delta^2(z-\lambda_k)\right\rangle\right\rangle_{\rm YM}.$$

Writing the condensate as integral over the density:

$$\langle\bar\psi\psi\rangle = \int d^2z\,\frac{\rho(z;\mu)}{z+m}.$$

How can the Silver Blaze effect traced back to the spectral function ?

For every fixed configuration at $\mu \neq 0$, the spectral density explicitely depends on μ.
When the gauge average ist taken, the average spectral density and any integral over it looses dependence on μ as long as $0 < \mu < m_B/3$. This is the Silver Blaze region.
The average spectral density is a complicated (weird !!!) function oscillating with amplitude $\propto e^{\Omega\mu}$, very rapidly with a period $1/\Omega$ (inverse space-time voume). Only when all is absolutely correctly integrated, the unwanted (wrong) μ-dependence will be cancelled.
This singular behavior has been studied by Osborn, Splittorff, Verbaarschot (in the years 2005 to 2008).
This is illustrated by a $0+1$ dimensional toy-model that can be followed in G. Aarts and K. Splittorff, JHEP 1008 (2010), arXiv:1006.0332

Outline

Return to the more realistic problem of phase diagram of 4-dimensional QCD

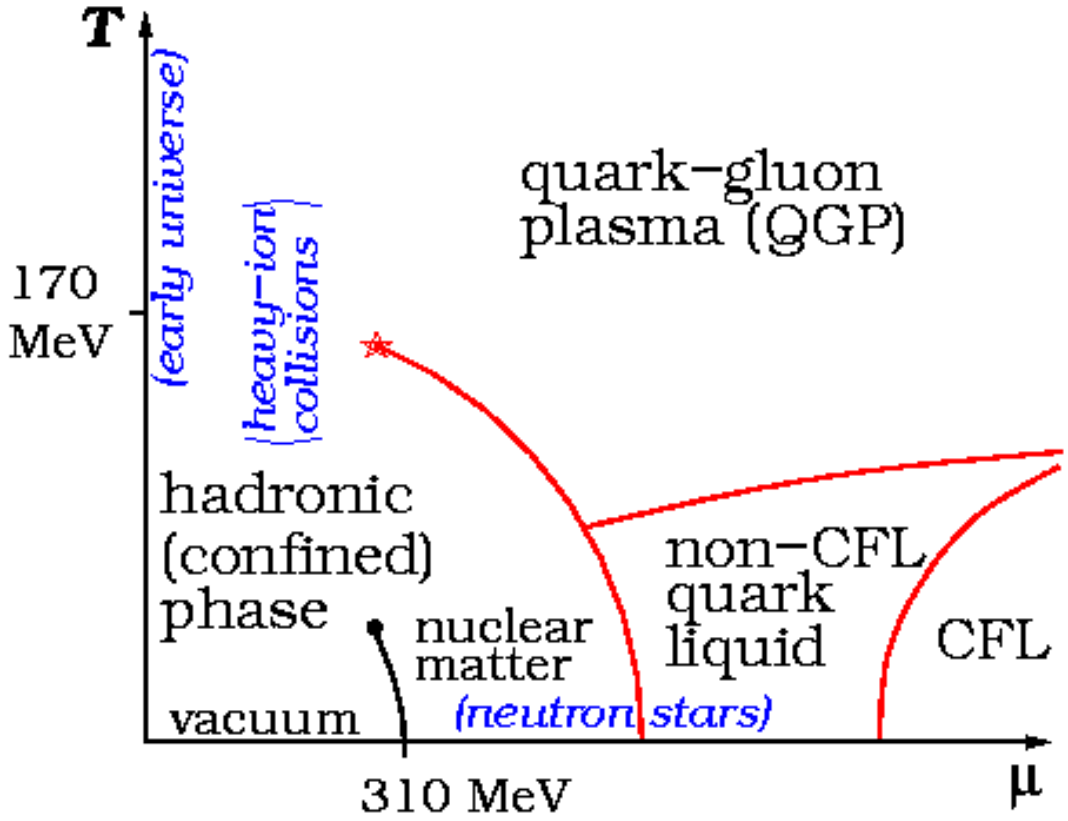

Figure: Conjectured phase diagram of QCD as a function of quark chemical potential μ and temperature T, from Wikipedia.

Minimalistic phase diagram

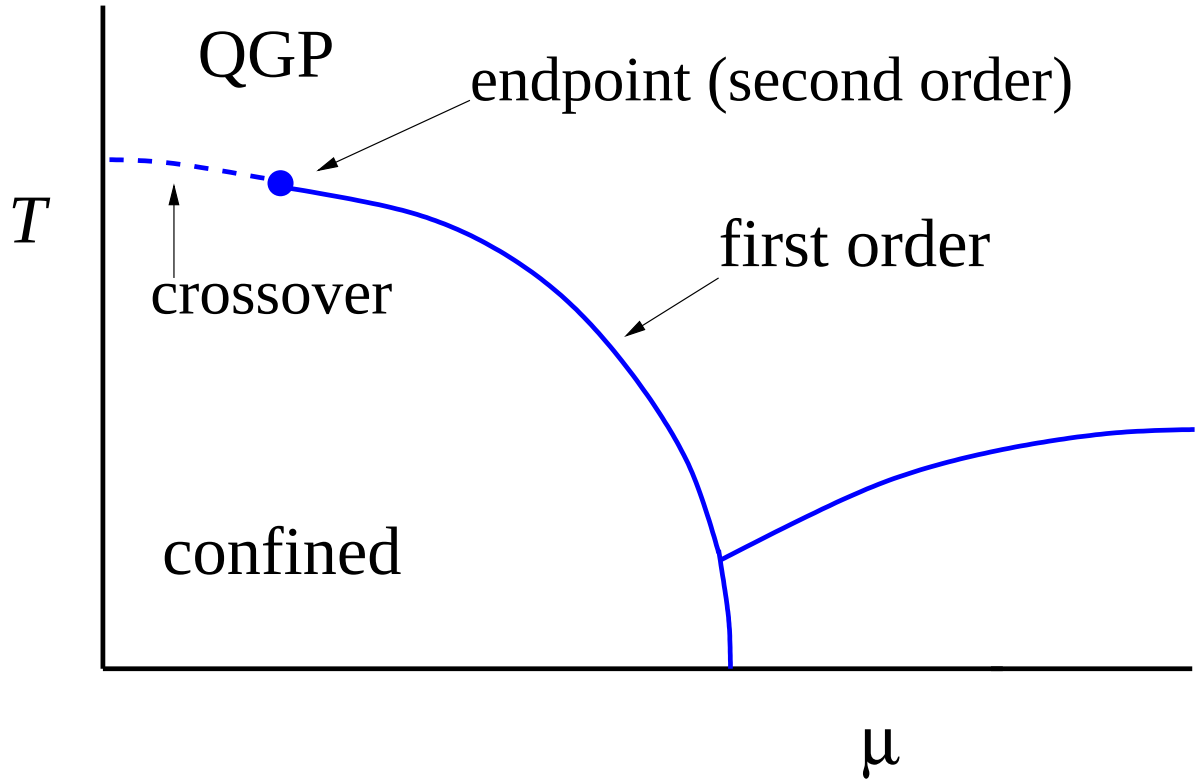

Figure: "Standard" phase diagram.

Curvature of the phase boundary near $\mu = 0$

For small chemical potential, the pseudo-critical temperature of the phase boundary at small nonzero μ can be written as a series in μ/T, for instance as

$$\frac{T_c(\mu)}{T_c(0)} = 1 + a_2 \left(\frac{\mu}{T_c(0)}\right)^2 + a_4 \left(\frac{\mu}{T_c(0)}\right)^4 + \dots$$

Since the partition function is an even function of μ, only even powers of μ appear.

FAQ : Curvature of the phase (crossover) boundary ?

Eventually not identical to the chemical freeze-out curve !!

The "sign problem" is hoped to be less severe for small μ and T close to the crossover at $T_c(0)$!

Once again about Reweighting

The general strategy in reweighting was already discussed above. The partition function is now written as

$$Z_w = \int DU\, w(U), \qquad w(U) \in \mathbf{C},$$

and observables are expressed as

$$\langle O \rangle_w = \frac{\int DU\, O(U) w(U)}{\int DU\, w(U)}.$$

Let us now introduce a new weight $r(U)$ ("r" resembling "reweighting" or "real"), which is chosen at will, such that

$$\langle O \rangle_w = \frac{\int DU\, O(U) \frac{w(U)}{r(U)} r(U)}{\int DU\, \frac{w(U)}{r(U)} r(U)} = \frac{\langle O \frac{w}{r} \rangle_r}{\langle \frac{w}{r} \rangle_r}.$$

Once again about reweighting

The average reweighting factor (w.r.t. the r ensemble) indicates the severity of the overlap problem.

$$\left\langle \frac{w}{r} \right\rangle_r = \frac{Z_w}{Z_r} = e^{-\Omega \Delta f}, \qquad \Delta f = f_w - f_r \geq 0,$$

where Ω denotes again the spacetime volume.
There is considerable freedom in choosing the new weight $r(U)$, provided that it has the interpretation of a probability weight, such that sampling (for the purpose of numerical simulation) is possible.

One may adapt the "model" r more successfully to the problem at hand, avoiding previous mistakes like in the phase-quenching case !

Two examples of reweighting strategies: Glasgow vs Budapest

- **Glasgow reweighting:** works at a fixed temperature (same lattice coupling β) and jumps in μ directly from 0 to the target μ,

$$\frac{w}{r} \sim \frac{\det M(U,\mu)}{\det M(U,\mu=0)},$$

  as illustrated in next Figure (left).
- However, this choice has a severe overlap problem, since the high-density phase is probed with a typical confinement ensemble at $\mu = 0$, just at the same temperature $T < T_c(\mu = 0)$ **below deconfinement.**
- The onset is not observed at $m_{\rm baryon}/3$ where it should be, but at $m_\pi/2$, similar to phase quenched simulations (i.e. there is no improvement over the previous quenched studies in valence approx.)

The Glasgow strategy fails for reasonable volumes

- One expects Δf to be large and hence the overlap problem will appear already on very small volumes (for example, a lattice volume 4^4).

The two reweighting strategies: Glasgow vs. Budapest

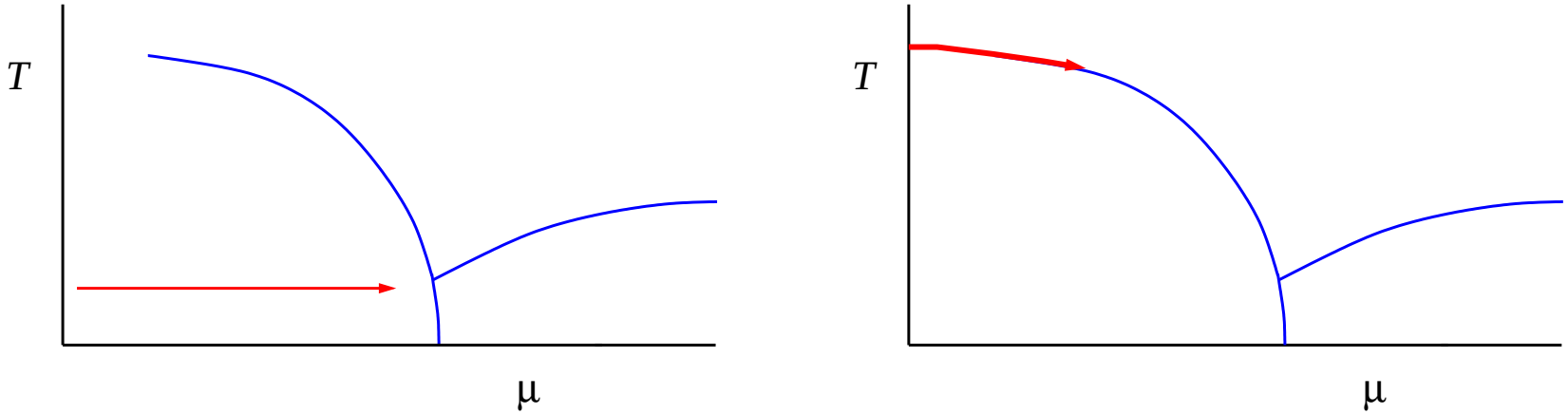

Figure: Reweighting at Fixed Temperature (Glasgow) (left) and Multiparameter Reweighting (Budapest), which is aiming to maximise the overlap as good as possible (right). Sampling of Budapest style proceeds at the reference point on the temperature axis and (very importantly !!!) successfully captures there a mixture of confining and deconfining configurations !

More precise about Budapest reweighting

Multiparameter/overlap preserving reweighting : here the temperature (or lattice coupling β) is adapted as well (see the last Figure, right). Hence

$$\frac{w}{r} \sim \frac{\det M(U,\mu)}{\det M(U,\mu=0)} e^{-\Delta S_{\rm YM}},$$

$$\Delta S_{\rm YM} = S_{\rm YM}(U,\beta) - S_{\rm YM}(U,\beta_c(\mu=0))$$

is the difference between gauge actions at the actual (T) and the reference temperature $T_{\rm ref} = T_c(\mu=0)$.

- The main idea here is the attempt to stay on the pseudo-critical line $T_c(\mu)$, improving overlap, since both the confined phase and the quark-gluon plasma are sampled, **albeit at higher T than really needed.**
- $T_c(\mu)$ is found by a T-scan (max. of susceptibility ?) at any fixed μ, regardless whether $\mu < \mu_E$ or $\mu > \mu_E$.

Imaginary chemical potential $\mu = i\mu_I$ shifts the quark condensate oppositely to real μ

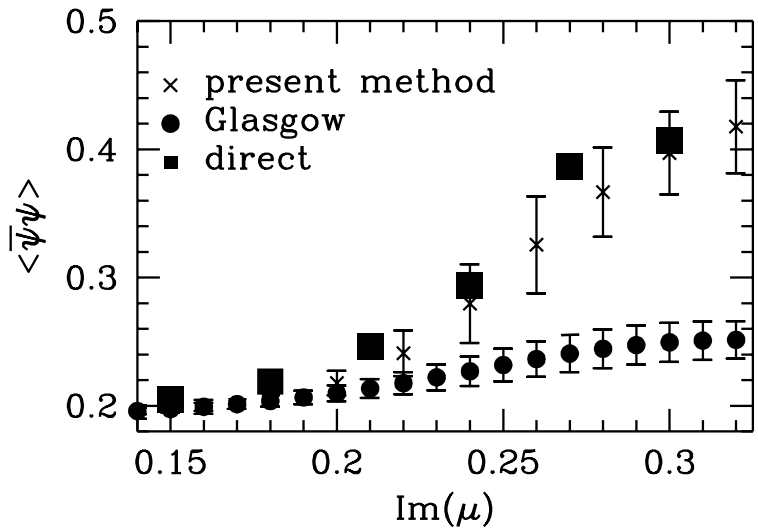

Figure: At imaginary chemical potential one can simulate ! Immediate simulation results (squares) can be compared with results of Glasgow-type (dots) and Budapest-type (crosses) reweighting. Glasgow reweighting is by far insufficient !

Critical endpoint from Budapest reweighting

μ_E and $T_E = T_c(\mu_E)$ denote the critical endpoint where the crossover line goes over into a first order line.
First, one has to find the line of maximal susceptibility (in other words, the ridge of the overlap measure).
The endpoint is fixed along the line of maximal susceptibility $\beta_{\max}(\mu)$ by an analysis of Lee-Yang zeroes: when to $\beta_{\max}$ an imaginary part β_I is added, the partition function develops a pattern of zeroes.

- If the location of the Lee-Yang-zero closest to the real axis moves towards the real axis in the limit $V \to \infty$, this tells us that one is sitting in the μ region related to the first order transition.
- If the location stays away from the real axis (independent of V), this is telling us that one is sitting in the μ region related to the crossover.

Lee-Yang zeros determining the endpoint of the first oder electroweak phase transition in a gauge-Higgs model

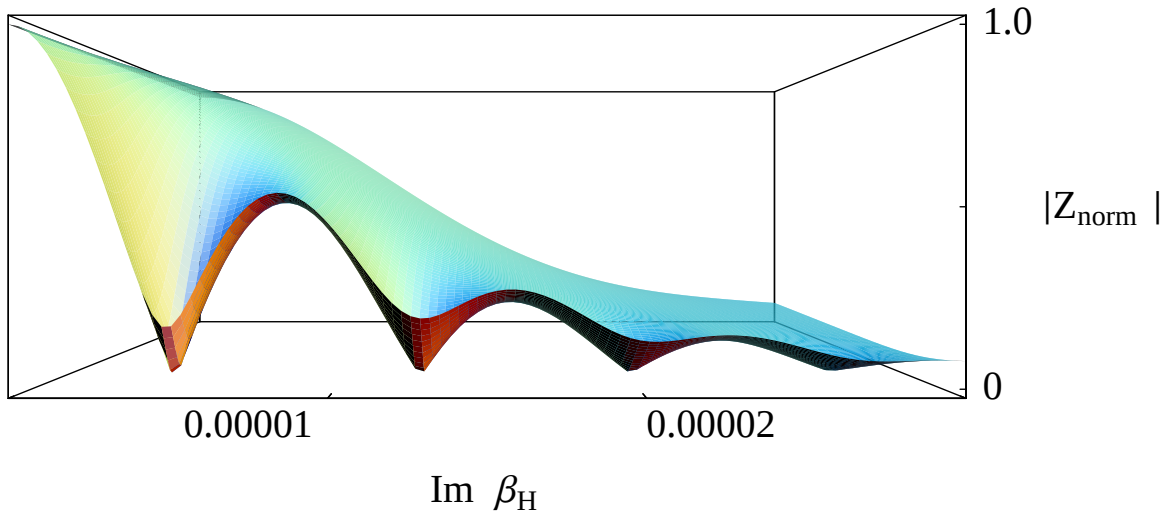

Figure: 3*d* view of $|Z_{\rm norm}|$ embracing the first zeroes found by adding $\mathrm{Im}\beta_G$ to real $\beta_G = 12$, at Higgs mass $M_H^* = 70$ GeV and for a volume 80^3 (Gürtler, Schiller, E.-M. I., 1997).

The Lee-Yang pattern locating the CEP at $\mu \neq 0$

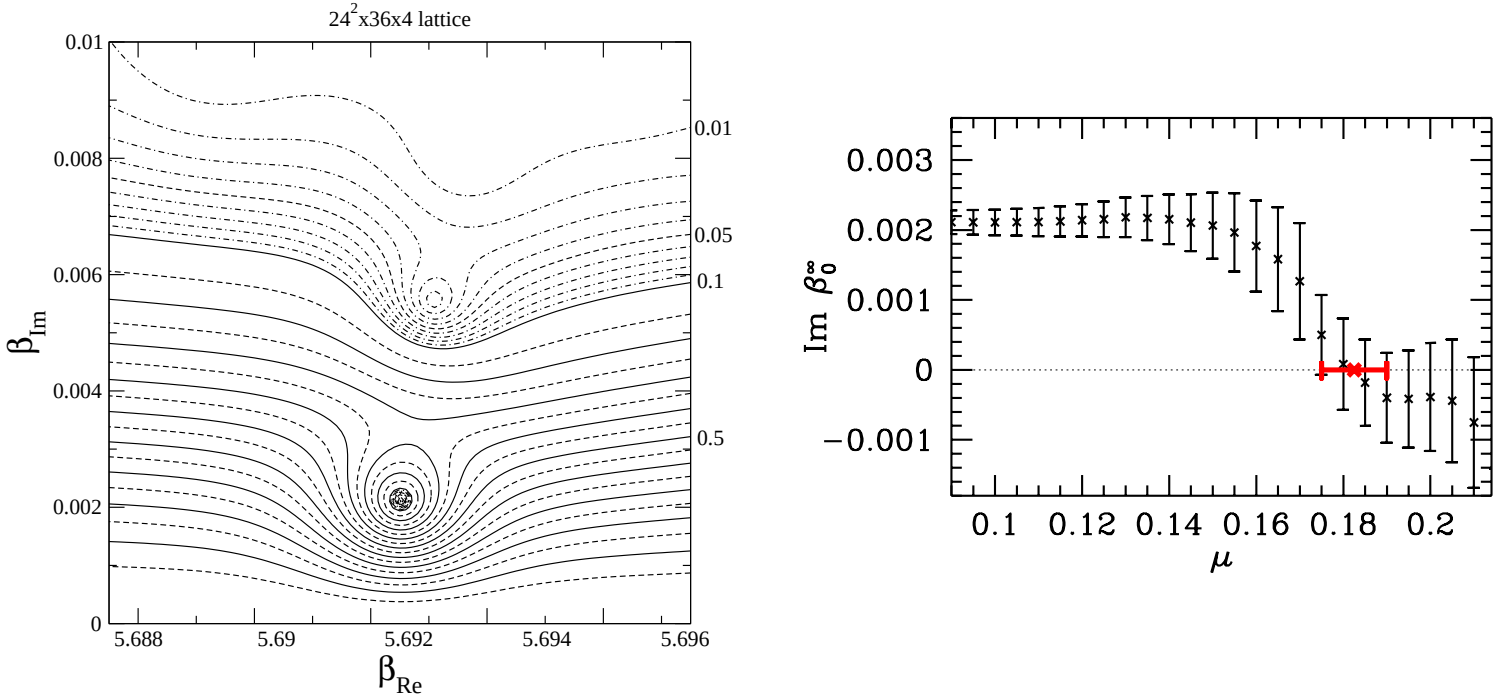

Figure: Lee-Yang Zeroes in the complex β plane, in the case of pure $SU(3)$ gauge theory (Ejiri 2006) (left) and the distance of the smallest Lee-Yang zero from the real axis as function of the chemical potential, in the case of full QCD (Fodor 2004) (right).

Fixing the critical endpoint CEP

This approach has led to a determination of the location of the critical endpoint for realistic quark masses (Fodor 2004):
(notice that quark number chemical potential $\mu^q = \mu^B/3$)

$\mu_E^q = 120(13)$ MeV, $T_E = 162(2)$ MeV, whereas $T_c(\mu^q = 0) = 164(3)$ MeV (see next Figure).

An earlier analysis with $3\times$ bigger quark masses and $3\times$ smaller volume (resulting in much heavier baryons !) had given (Fodor 2003): (with twice as high μ_E^q !)

$\mu_E^q = 241(31)$ MeV, $T_E = 160(4)$ MeV, whereas $T_c(\mu^q = 0) = 172(3)$ MeV.

Status of the Multiparameter Reweighting strategy

The final multiparameter reweighting result was obtained using $N_f = 2 + 1$ quark flavors with physical quark masses on a coarse lattice with only $N_\tau = 4$ time slices. $a \approx 1/(4 \times 160\ \mathrm{MeV}) \approx 0.25\ \mathrm{fm}$.

Unfortunately, this method is very expensive to extend to smaller lattice spacing (larger N_τ) and it has not been repeated attempting to approach the continuum limit.

A critical analysis has been presented by Splittorff (2006).

Critical endpoint (μ_E, T_E)

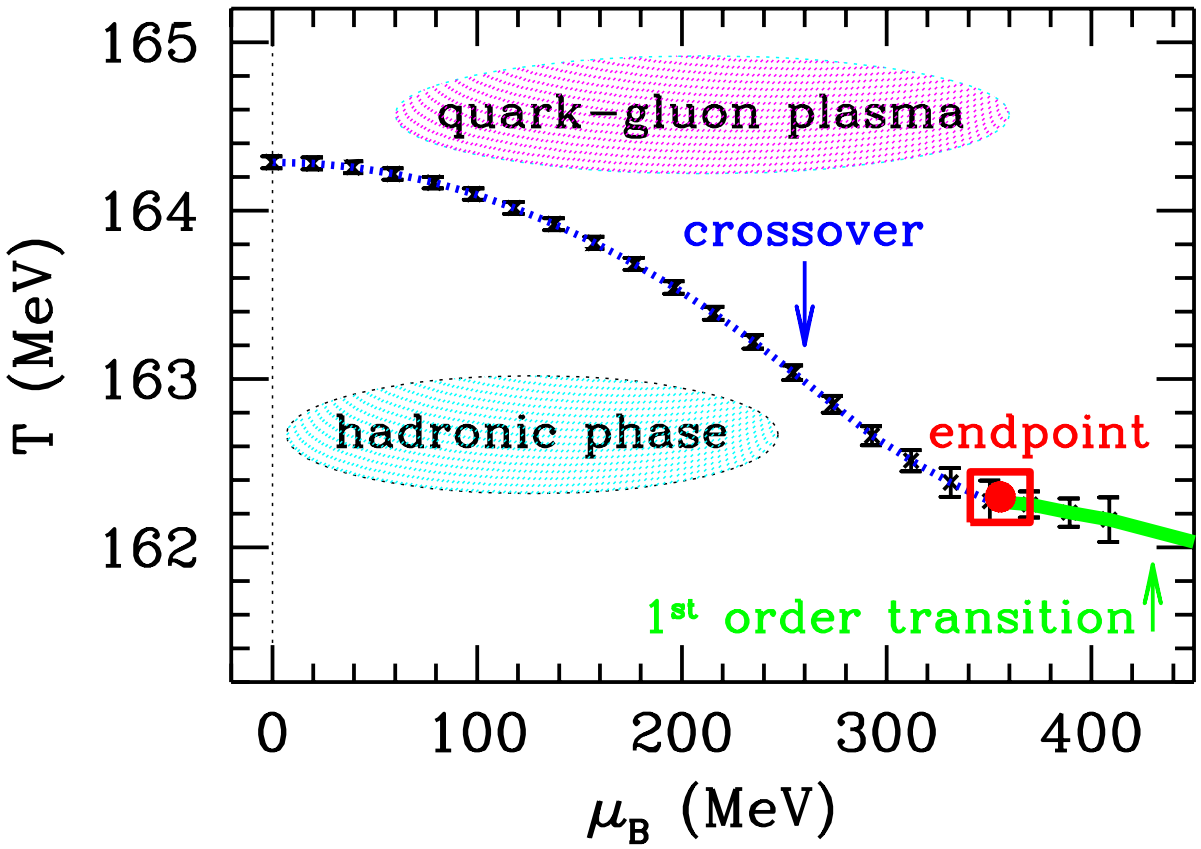

Figure: Left: Location of the critical endpoint for $N_f = 2 + 1$ using multi-parameter/overlap preserving reweighting, on a lattice with $N_\tau = 4$ (Fodor 2004).

The use of multiparameter reweighting

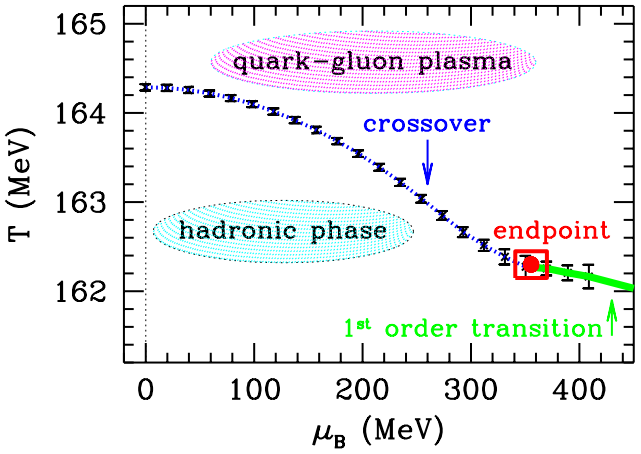

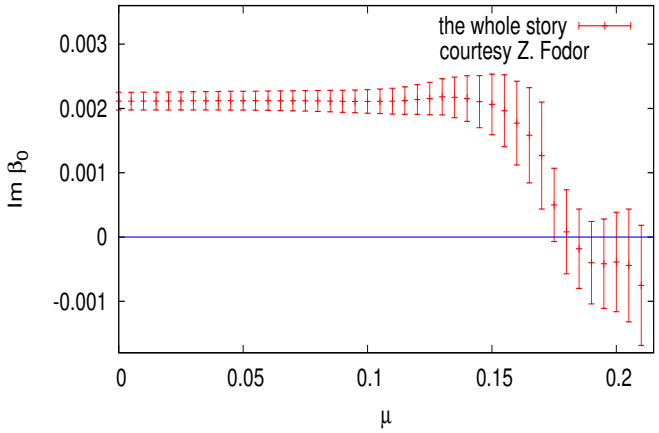

Figure: *Left*: QCD phase diagram from Fodor (2004) obtained by combined reweighting in μ and β of the $\mu = 0, \beta = \beta_c$ reference ensemble (blue dot). *Right*: improved data illustrating the insensitivity of $\mathrm{Im}\beta_{\mathrm{LY}}$ relative to μ, followed by an abrupt change.

Height lines of the average phase factor in the matrix model of Han and Stephanov

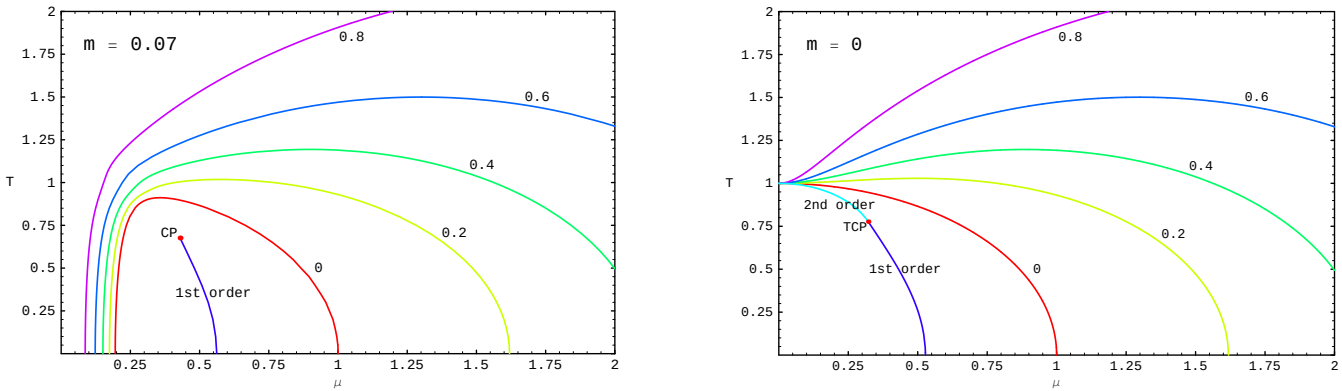

Figure: Height lines of the average sign in the μ–T plane for the random matrix model of Han and Stephanov (2008) designed to describe the transition and the sign problem (2008). **Left:** Contours of average phase factor for $m = 0.07$ with first-order line and critical endpoint CEP. **Right:** Contours of average phase factor for the chiral limit $m = 0$. First-order line, chiral symmetry second-order transition line and tricritical point TCP are shown.

The matrix model of Han and Stephanov for dense QCD (arXiv:0805.1939)

$$Z_{N_f} = \int \mathcal{D}X \, e^{-N \mathrm{Tr}\, XX^\dagger} \det{}^{N_f} \mathbb{D} = \langle \det{}^{N_f} \mathbb{D} \rangle_X \, ,$$

where $\mathbb{D}$ is the $2N \times 2N$ matrix approximating the Dirac operator:

$$\mathbb{D} = \begin{pmatrix} m & iX + C \\ iX^\dagger + C & m \end{pmatrix} ,$$

with

$$C = \mu \mathbb{1}_N + iT \begin{pmatrix} \mathbb{1}_{N/2} & 0 \\ 0 & -\mathbb{1}_{N/2} \end{pmatrix} .$$

The scenarios predicted by the model of Han and Stephanov

Two scenarios are predicted by the model:

- first order line with critical endpoint for quark mass away from chiral limit
- first order line separated from second order line (extending to $\mu = 0$) for the chiral limit (zero quark mass)

In each case, the height line of $R = 0$ keeps the phase transitions separated (not accessible by extrapolation) from the rest of the μ–T plane.

The average phase factor in the matrix model of Stephanov

The leading exponential behavior of the partition functions Z_{1+1} and Z_{1+1^*} is the same, it will cancel in the ratio R. Taking into account preexponential factors (determined by the second order derivatives of the potential function $\Omega_{1+1}(A)$ and $\Omega_{1+1^*}(A)$ with respect to all elements of flavor matrix A) :

$$Z_Q \overset{N\to\infty}{\to} \left(\frac{2\pi}{N}\right)^4 \left(\det \Omega''_Q\right)^{-\frac{1}{2}} e^{-N\Omega_Q(A)}\Big|_{A=A_{saddle}} ,$$

where Q indicates the respective quark content of the theory, $1+1$ or $1+1^*$, and

$$\det \Omega''_Q \equiv \det\left(\frac{\partial^2 \Omega_Q}{\partial A_\alpha \partial A_\beta}\right) .$$

The average phase factor in the matrix model of Stephanov

Finally, the average phase factor is given by

$$R \equiv \langle e^{2i\theta} \rangle_{1+1^*} = \frac{Z_{1+1}}{Z_{1+1^*}} = \left[\frac{\det \Omega''_{1+1}}{\det \Omega''_{1+1^*}} \right]^{-\frac{1}{2}} = \left. \frac{u^2 - v^2}{x^2 - y^2} \right|_{A=A_{saddle}}$$

with u, v, x and y depending on m, T, μ and the saddlepoint equation.

A more intuitive "overlap measure": α

α is defined as the fraction of sampled configurations that contributes the biggest contributions (amounting to a fraction $1-\alpha$) to the average sign (total weight contributed to the target ensemble).

The reweighting step should not be too small and not too big ! Therefore the optimal overlap is $\alpha = 50$ percent.

The height lines of the overlap measure α in the β–μ plane show clearly, where one can rely on reweighting.

The grey area is not accessible by reweighting from the reference point located at $\beta = \beta_c(\mu = 0)$ at $\mu = 0$.

The ridge of the susceptibility (usually locating the crossover line) falls on top of the ridge of the overlap measure α.

The half width in μ of the ridge, $\mu_{1/2}$, defined by $\alpha = 0.5$, shrinks with increasing volume like $\mu_{1/2} \sim V^{-\gamma}$ with $\gamma \approx 1/3$.

Height lines of the overlap measure α

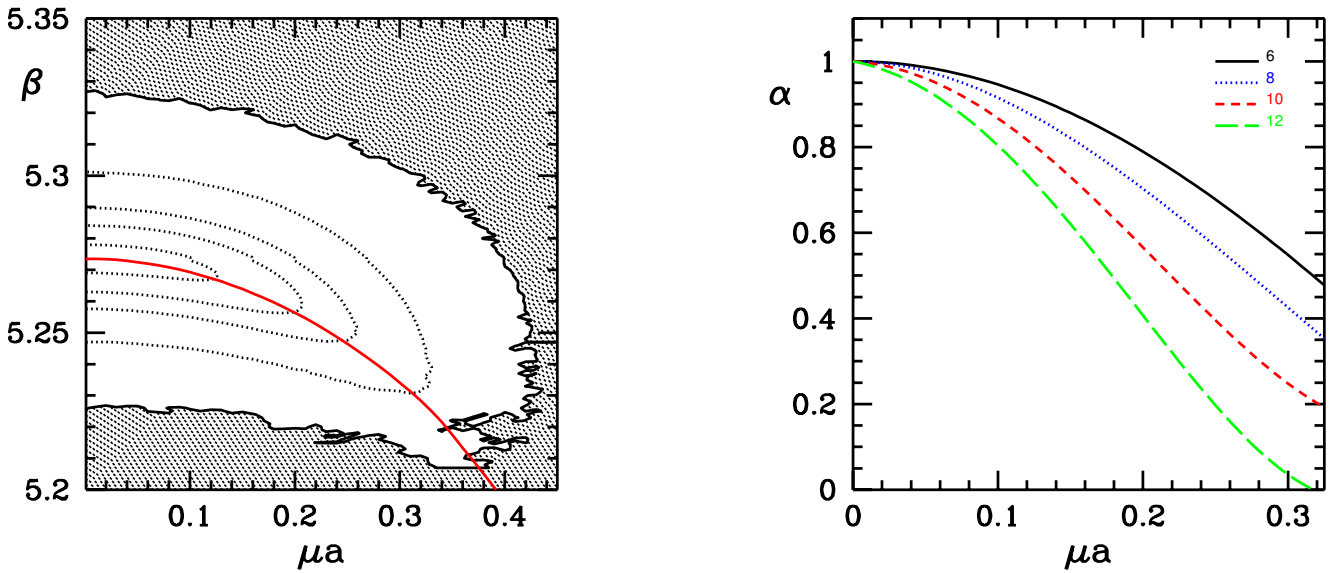

Figure: (a) The left panel shows the real μ–β plane. 33000 configurations were simulated at the parameter set: $\beta = 5.274$, $m_{u,d} = 0.096$, $m_s = 2.08 m_{u,d}$ on a $4 \cdot 8^3$ size lattice. This is $\beta_c(\mu = 0)$ in the $N_f = 2 + 1$ case. The dotted lines are contours of constant overlap. The dotted area is the unknown territory where the overlap vanishes. The solid line is the phase transition/crossover line determined by the peaks of susceptibility. (b) In the right panel the volume and the μ dependence of the overlap α is shown. Upper curves correspond to smaller lattice sizes, $4 \cdot 6^3$, $4 \cdot 8^3$, $4 \cdot 10^3$ and $4 \cdot 12^3$ respectively. The half width $\mu_{1/2}$ scales as indicated.

Phase boundary obtained by different methods

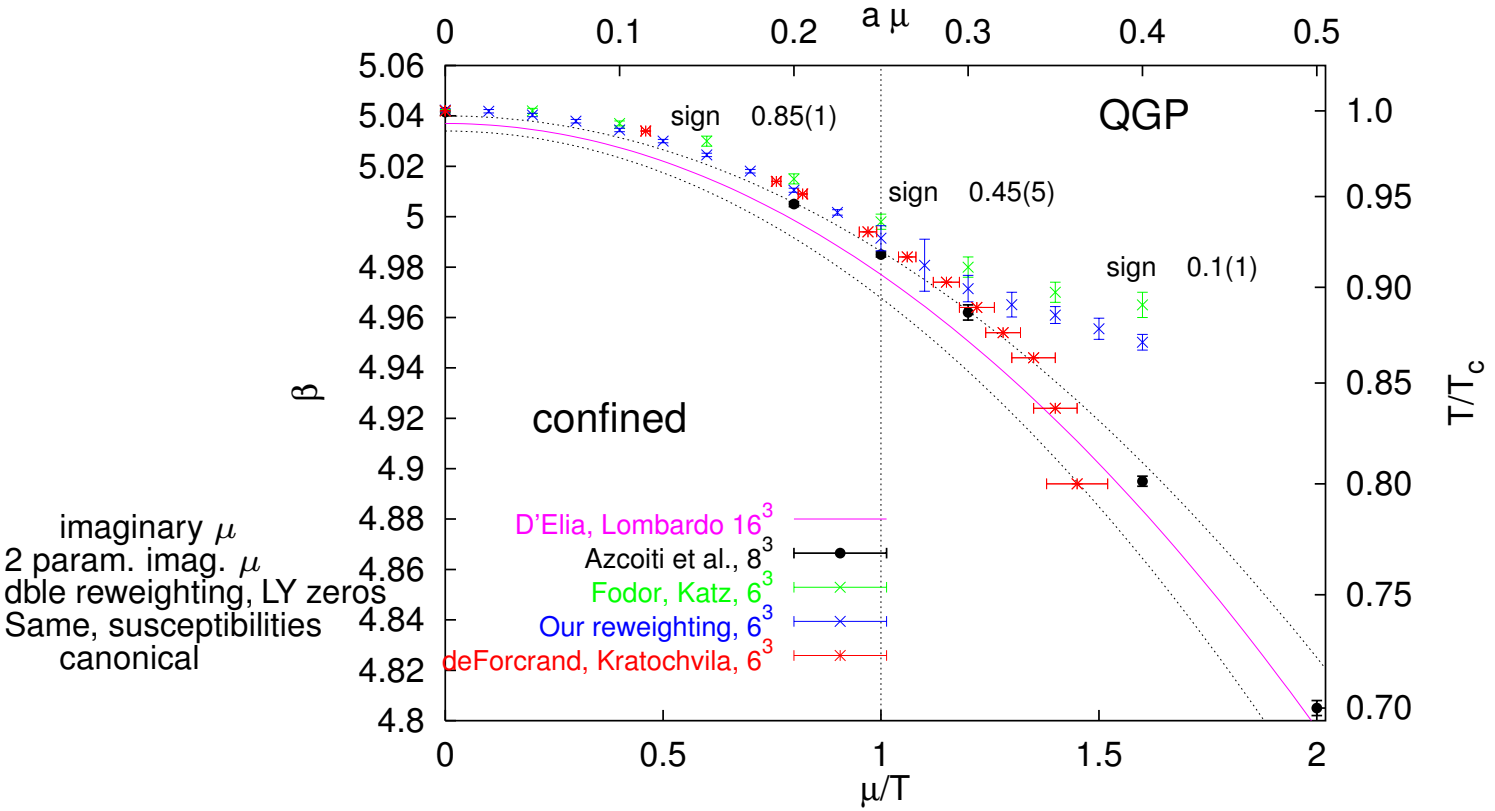

Figure: Pseudo-critical temperature determined by various approaches for the same lattice theory (4-flavor staggered quarks with mass $am = 0.05$ on an $N_t = 4$ lattice) (Kratochvila 2005). All approaches agree among each other for $\mu/T \lesssim 1$.

Outline

Taylor expansion of log det M

An alternative, and more modest, idea relies on a Taylor series expansion of the logarithm of the determinant in μ/T around $\mu = 0$. It applies to the full interior of the phase diagram. The coefficients of the expansion can be calculated using conventional simulations at $\mu = 0$, where the sign problem is fortunately absent. This approach is continuously pursued by several groups: Allton (2002), Gavai (2004), Allton (2005), Kaczmarek (2011), Endrodi (2011), Borsanyi (2012).

A recent review can be found in S. Borsanyi, arXiv:1511.06541 (Lattice 2015)

Taylor expansion of the pressure

We start from the grand-canonical ensemble, considering the pressure,

$$p(T,\mu) = \frac{T}{V} \ln Z.$$

Since the pressure is an even function of μ, one can write

$$\Delta p(T,\mu) \equiv p(T,\mu) - p(T,0) = \frac{\mu^2}{2!}\frac{\partial^2 p}{\partial \mu^2}\Big|_{\mu=0} + \frac{\mu^4}{4!}\frac{\partial^4 p}{\partial \mu^4}\Big|_{\mu=0} + .$$

$p(T,\mu=0)$ is obtained from the "interaction measure" a.k.a. the "trace anomaly", evaluated at $\mu = 0$.

The pressure evaluated at $\mu = 0$

The quantity $I(T) = \epsilon(T, \mu = 0) - 3p(T, \mu = 0)$ is related to a total derivative w.r.t. T :

$$\frac{I(T)}{T^5} = \frac{d}{dT}\frac{p(T, \mu = 0)}{T^4}.$$

The l.h.s. quantity is called "trace anomaly", *alias* "interaction measure". This relation can be integrated giving the EoS at $\mu = 0$

$$\frac{p(T, \mu = 0)}{T^4} - \frac{p(T_0, \mu = 0)}{T_0^4} = \int_{T_0}^{T} dT' \frac{I(T')}{T'^5}$$

Trace anomaly as (subtracted) lattice expectation value

The integrand (trace anomaly) expresses the lattice-scale-dependence of the lattice action.

$$\frac{I(T)}{T^4} = -\frac{1}{T^3 V}\left\langle \frac{d\ln Z}{d\ln a}\right\rangle\Big|_{\rm sub}$$

with action with different coupling parameters b_i

$$S = \sum b_i S_i \qquad (3)$$

$$\frac{I(T)}{T^4} = \frac{1}{T^3 V}\sum_i \frac{db_i}{da}\left\langle \frac{\partial S}{\partial b_i}\right\rangle\Big|_{\rm sub}$$

with subtracted expectation values

$$\left\langle \dots \right\rangle\Big|_{\rm sub} = \left\langle \dots \right\rangle\Big|_{\text{finite T lattice}} - \left\langle \dots \right\rangle\Big|_{\text{T=0 lattice}}$$

The pressure evaluated at zero baryon density

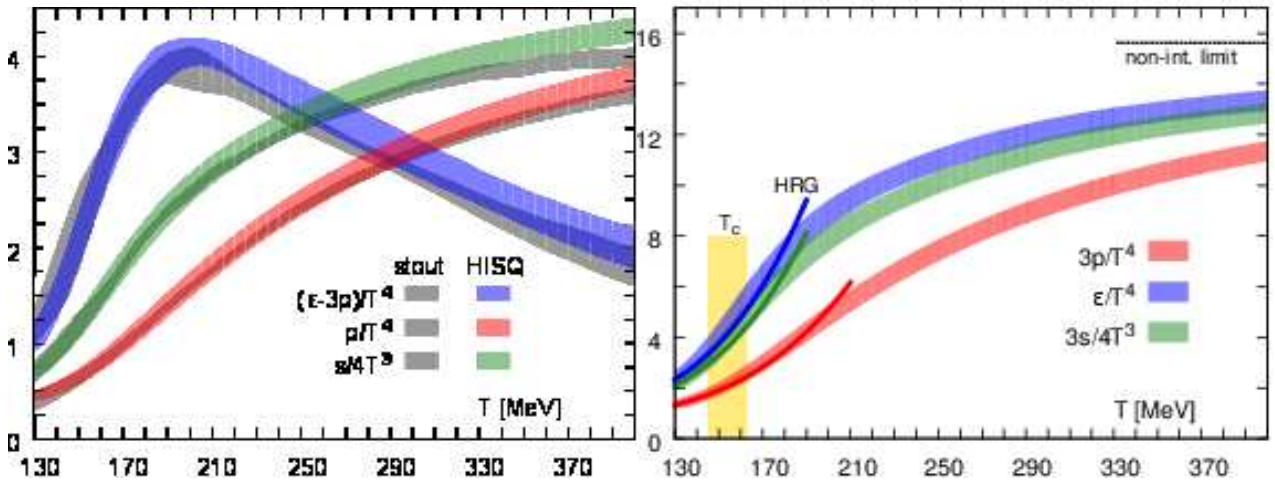

Figure: (Left) Comparison of the trace anomaly $(\epsilon - 3P)/T^4$, pressure and entropy density calculated with the HISQ (colored) (Bazavov 2014) and stout scheme (grey) (Borsanyi 2013) for staggered fermions. (Right) Continuum extrapolated results for pressure, energy density and entropy density at $\mu = 0$ obtained with the HISQ action (Bazavov 2014). Solid lines on the low temperature side correspond to results obtained from HRG model calculations.

Taylor expansion of the pressure in μ

More compactly,

$$\frac{\Delta p(\mu)}{T^4} = \sum_{n=1}^{\infty} c_{2n}(T) \left(\frac{\mu}{T}\right)^{2n}.$$

The coefficients c_{2n} are defined at $\mu = 0$. Note that the other thermodynamic quantities follow immediately from these coefficients, for example the density is given by

$$\langle n(\mu) \rangle = \frac{\partial p}{\partial \mu} = 2T^3 \sum_{n=1}^{\infty} n c_{2n}(T) \left(\frac{\mu}{T}\right)^{2n-1}.$$

Estimate of the convergence radius r ?

$$r = \lim_{n\to\infty} \sqrt{\left|\frac{c_{2n}}{c_{2n+2}}\right|}(T_E) \qquad (4)$$

Can this give $r = \frac{\mu_E}{T_E}$? This would require large orders !

Example for Taylor series expansion

In order to see what it is needed in practice, it is useful to give some explicit expressions. We start from

$$Z = \int DU \, (\det M)^{N_f} \, e^{-S_{\rm YM}} = \int DU \, e^{-S_{\rm YM} + N_f \ln\det M(\mu)} .$$

Differentiation is straightforward and

$$\frac{\partial \ln Z}{\partial \mu} = \left\langle N_f \frac{\partial}{\partial \mu} \ln\det M \right\rangle ,$$

$$\frac{\partial^2 \ln Z}{\partial \mu^2} = \left\langle N_f \frac{\partial^2}{\partial \mu^2} \ln\det M \right\rangle + \left\langle \left(N_f \frac{\partial}{\partial \mu} \ln\det M \right)^2 \right\rangle - \left\langle N_f \frac{\partial}{\partial \mu} \ln\det M \right\rangle^2 ,$$

etc

Example for Taylor series expansion

Writing $\ln\det M = \mathrm{Tr}\,\ln M$, these can be expressed in terms of traces

$$\frac{\partial}{\partial\mu}\ln\det M = \mathrm{Tr}\,M^{-1}\frac{\partial M}{\partial\mu},$$

$$\frac{\partial^2}{\partial\mu^2}\ln\det M = \mathrm{Tr}\,M^{-1}\frac{\partial^2 M}{\partial\mu^2} - \mathrm{Tr}\,M^{-1}\frac{\partial M}{\partial\mu}M^{-1}\frac{\partial M}{\partial\mu},$$

etc., allowing for an easy diagrammatic interpretation.
It is straightforward to work out more derivatives, but the number of terms increases rapidly.

Moreover, there are again cancelations required: the pressure p is an intensive quantity, and hence the coefficients c_{2n} must be finite in the thermodynamical limit. However, the individual contributions may scale differently, as is clear from the explicit expressions above.

A concrete representation for the leading and next-to-leading order

$$\frac{p(T,\mu_B)-p(T,0)}{T^4} = \frac{1}{2}\,\chi_2^B(T)\left(\frac{\mu_B}{T}\right)^2 \times\left(1+\frac{1}{12}\frac{\chi_4^B(T)}{\chi_2^B(T)}\left(\frac{\mu_B}{T}\right)^2\right)+\mathcal{O}(\mu_B^6)$$

χ_n^B are the cumulants.

Leading order and next-to-leading order

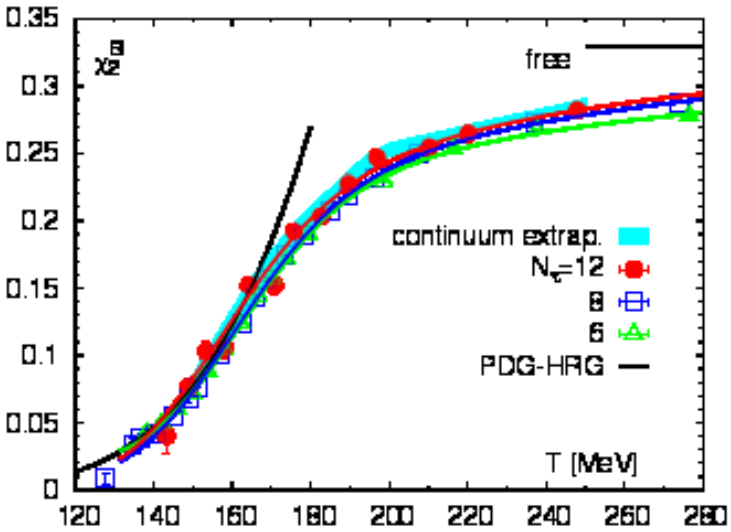

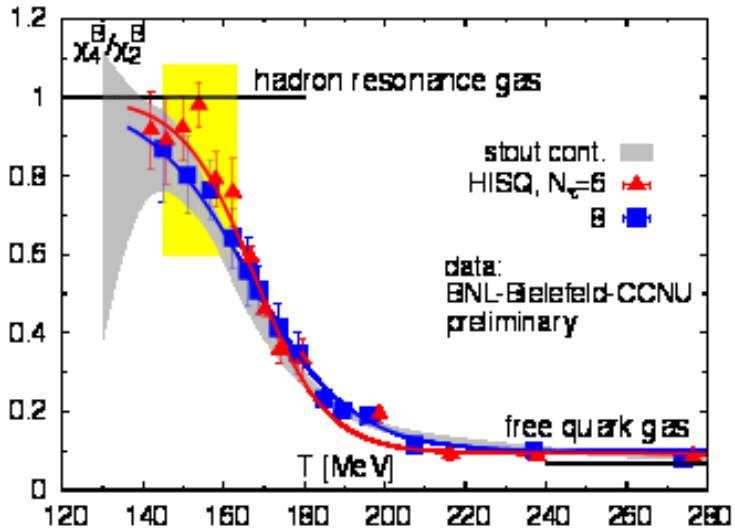

Figure: Expansion coefficients of the pressure at non-zero baryon chemical potential. The left hand figure shows the leading order correction (Bazavov 2012) and the right hand figure shows the relative contribution of the next to leading order correction. The continuum extrapolated result obtained with the stout action is taken from (Borsanyi 2013).

Other thermodynamical functions

$$\frac{p(T,\mu)}{T^4} = \sum_{i,j,k=0}^{\infty} \frac{\chi_{ijk}}{i!j!k!} \left(\frac{\mu_B}{T}\right)^i \left(\frac{\mu_Q}{T}\right)^j \left(\frac{\mu_S}{T}\right)^k \rightarrow \sum_{n=0}^{\infty} c_n \left(\frac{\mu_B}{T}\right)^n$$

$$\frac{\epsilon(T,\mu)}{T^4} = \sum_{n=0}^{\infty} \left(\frac{\mu_B}{T}\right)^n \left(T\frac{dc_n}{dT} + 3c_n\right)$$

$$\frac{s(T,\mu)}{T^3} = \sum_{n=0}^{\infty} \left(\frac{\mu_B}{T}\right)^n \left(T\frac{dc_n}{dT} + (4-n)c_n\right)$$

Main contributions to p from second-order susceptibilities.
4-th order corrections important closer to the "transition",
partly because the T-derivative of c_4 is large there.

Other thermodynamical functions

quark density = baryon density/3 :

$$\frac{n_q}{T^3} = 2c_2\frac{\mu}{T} + 4c_4\left(\frac{\mu}{T}\right)^3 + 6c_6\left(\frac{\mu}{T}\right)^5 + \ldots$$

quark number susceptibility :

$$\frac{\chi_q}{T^2} = 2c_2 + 12c_4\left(\frac{\mu}{T}\right)^2 + 30c_6\left(\frac{\mu}{T}\right)^4 + \ldots$$

Problems/successes for the Taylor series expansion

Most current work focuses on going closer to the continuum limit for physical quark masses. An example is given in the following figure (Borsanyi 2012): plotted is a continuum estimate of the pressure as a function of temperature for two values of μ_L, the baryon chemical potential for the two light flavors.

There is apparently hardly need to go beyond $\mathcal{O}(\mu_B^4)$ at $\mu_B \approx 400..450$ MeV
(provided by Hegde 2014 [at "Quark Matter" Darmstadt]).

Note that in the following figure only the leading (second order) $\mathcal{O}(\mu_L^2)$ contribution is included.

The pressure for $\mu \neq 0$ vs. $\mu = 0$, comparing lattice (in continuum extrapolation) with HRG

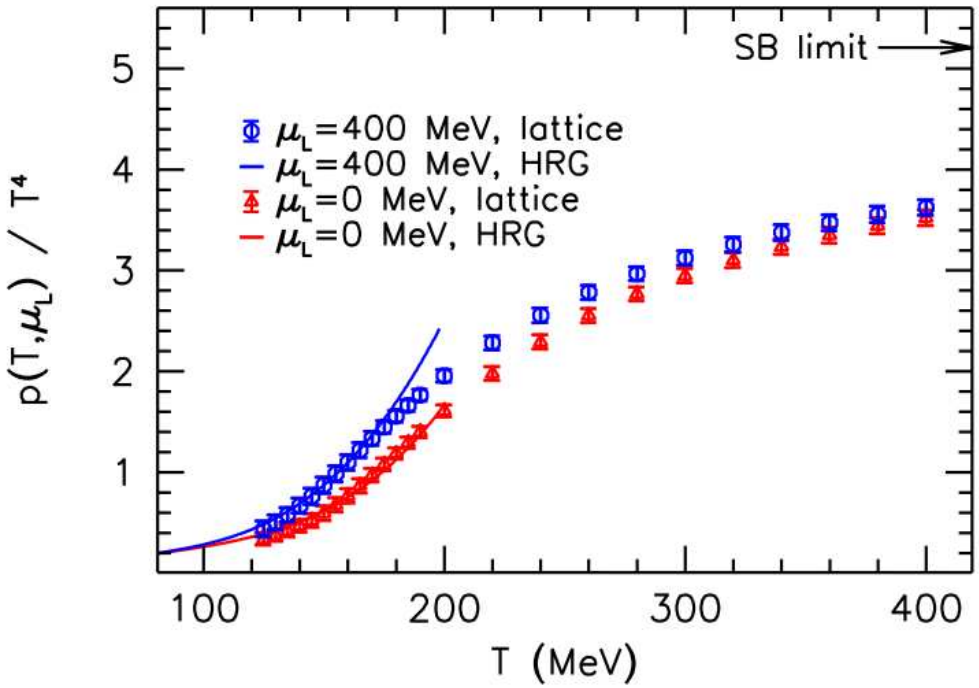

Figure: Continuum estimate of the pressure as a function of temperature for $\mu_l = 0$ and $\mu_l = 400$ MeV (of *u* and *d* quarks), only including the term up to $\mathcal{O}(\mu_l^2)$, for $N_f = 2 + 1$ flavors of quarks with physical masses, using a continuum extrapolation (Borsany 2012). HRG means "hadron resonance gas model".

The first coefficients of the Taylor expansion

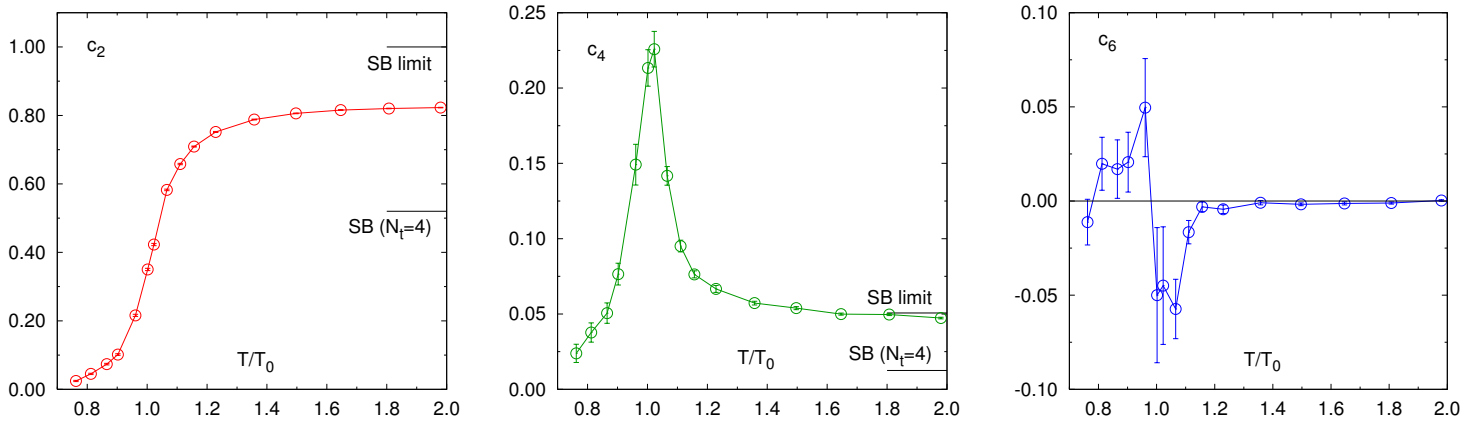

Figure: First three coefficients in the Taylor expansion of the QCD pressure versus $T/T_c(\mu = 0)$ (from C. Schmidt 2006). They all show a characteristic behavior at the temperature $T = T_c(\mu = 0)$. One sees that the quark number susceptibility evaluated at $\mu = 0$ is a good deconfinement order parameter (could replace the Polyakov loop) ! The coefficient c_4 is well resembling the Polyakov loop susceptibility.

The quark number susceptibility extended to non-zero μ

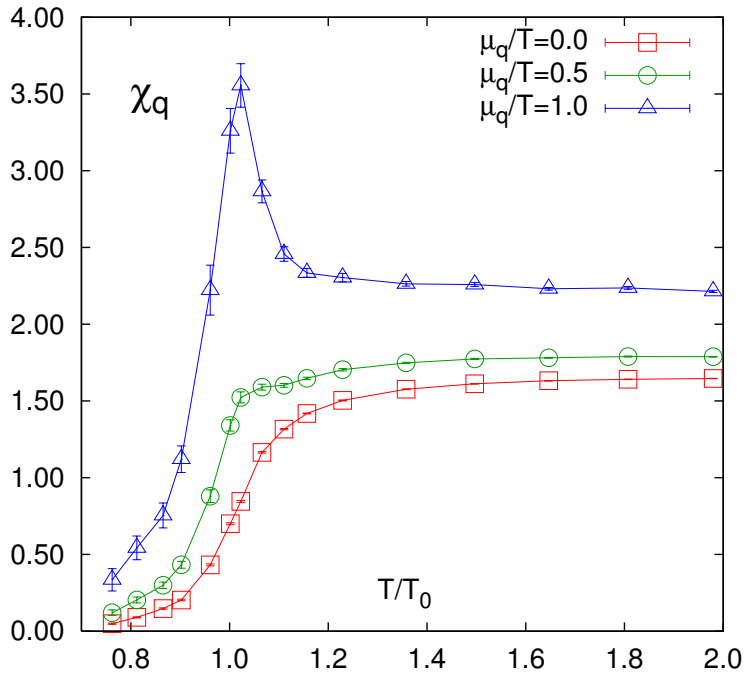

Figure: The quark number susceptibility at zero and non-zero μ (Schmidt 2006)

Outline

Phase boundary

The compilation of results for the phase boundary using various methods presented before (de Forcrand 2010) is rather old. Nevertheless, it shows the essential findings.
Good agreement exists between the various methods as long as $\mu/T \lesssim 1$, for which the average sign is clearly different from zero, at least on the small spatial volume sizes and fixed $N_\tau = 4$ considered at this time.
However, as the chemical potential is increased, the average sign becomes zero within errors, and the results from the various approaches start to deviate. Which result is correct, if any, cannot be concluded.
Hence it is the "sign problem" which was preventing further progress.

Latest developments concerning the phase boundary

In more recent years the attention has shifted to the determination of the lowest-order coefficients in the (imaginary μ) expansion to higher precision than before, i.e. for physical quark masses and closer to the continuum limit.

A relatively new paper (D'Elia, PoS(LATTICE 2014 (2015)020, arXiv:1502.06047) gives a summary for results for the second-order coefficient κ in the expansion

$$\frac{T_c(\mu_B)}{T_c} = 1 - \kappa \left(\frac{\mu_B}{T_c}\right)^2 + \mathcal{O}\left(\mu_B^4\right). \qquad (5)$$

It is found that $0.007 \lesssim \kappa \lesssim 0.018$, depending on the method used.

NB.: This paper considers also simulations with θ-term and external electromagnetic fields !

Latest developments concerning the phase boundary

Most results have been obtained still away from the continuum limit and hence it is expected that a unique answer will emerge subsequently from this activity.
The state-of-the-art has recently been summarised in S. Borsanyi, arXiv:1511.06541 (Lattice 2015)

Where do we know from how large μ can be expected at NICA ?

From central Pb+Pb (Au+Au) collisions at SIS, AGS, SPS and RHIC, the collision energy dependence of temperature and baryonic chemical potential (appearing in the chemical composition of the particle yields, say through THERMUS) has been found.

The collision energy dependence of temperature and chemical potential at chemical freeze-out

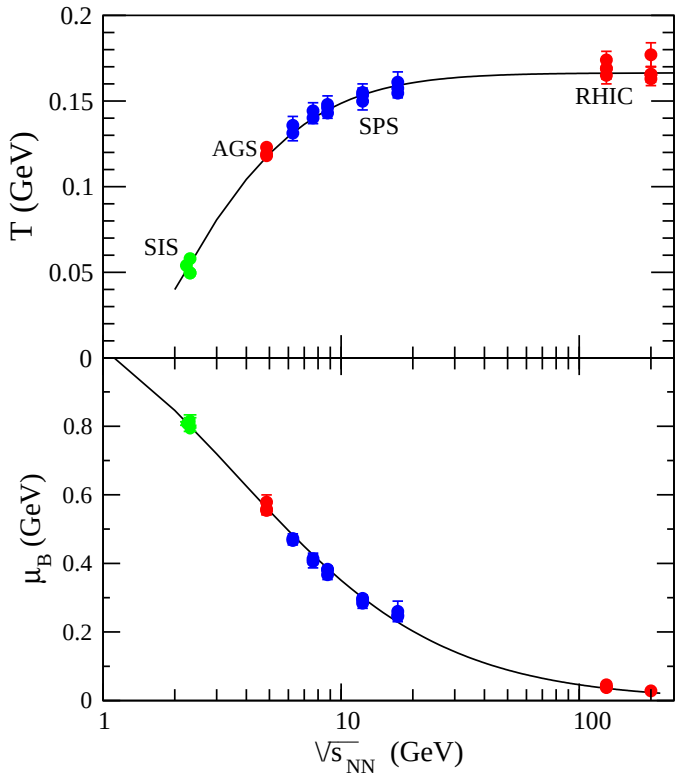

Figure: Energy dependence of the chemical freeze-out parameters T and μ_B.

The collision energy dependence of the chemical potential

$$\mu_B = 3\mu_q = \frac{1.308}{1 + 0.273\sqrt{s_{NN}}}$$

This μ_B enters the (chemical) freeze-out temperature $T_{\rm freeze}(\mu_B)$ close to the crossover (at $\mu_B = 0$ and $T_c(\mu = 0) = 0.166$ GeV which is parametrized as follows

$$\frac{T_{\rm freeze}}{T_c(\mu = 0)} = 1 - 0.023 \left(\frac{\mu_B}{T}\right)^2 - \mathcal{O}(\left(\frac{\mu_B}{T}\right)^4)$$

J. Cleymans et al. Phys. Rev. C 63 (2006) 034905

For comparison: the chemical freeze-out curve

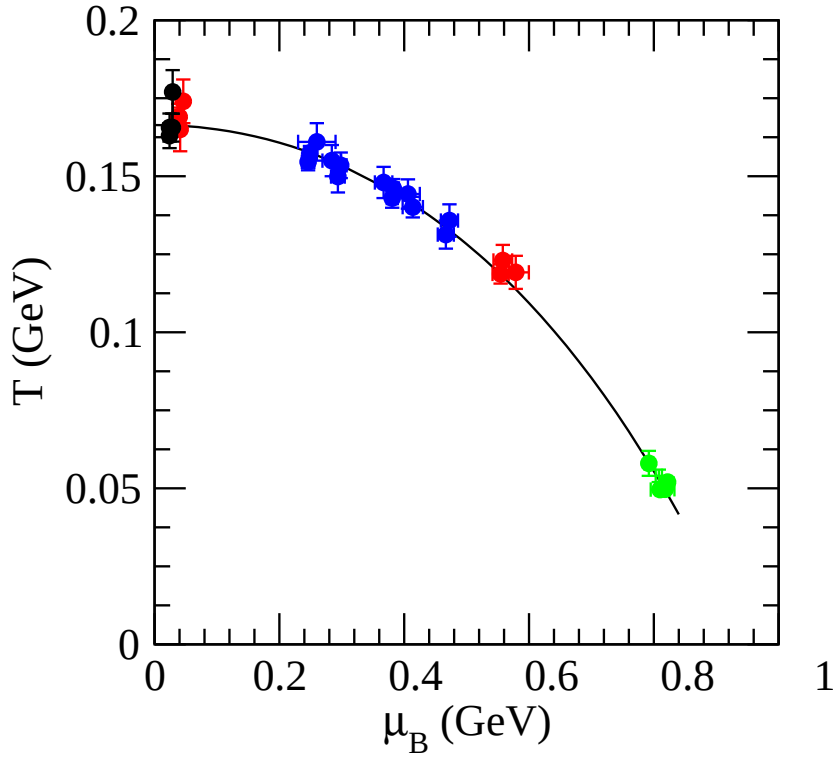

Figure: Values of μ_B and T for different collision energies. The solid line is a parameterization corresponding to $T(\mu_B) \approx 0.17 - 0.13\mu_B^2 - 0.06\mu_B^4$.

For comparison: the chemical freeze-out curve

- This curvature is much bigger (three times bigger) than the curvature of the crossover.
- Thus, the freeze-out is far from the eventual Critical Endpoint.
- The freeze-out curve is entirely embedded in the hadron gas phase.

EoS : The μ-dependent part of the pressure

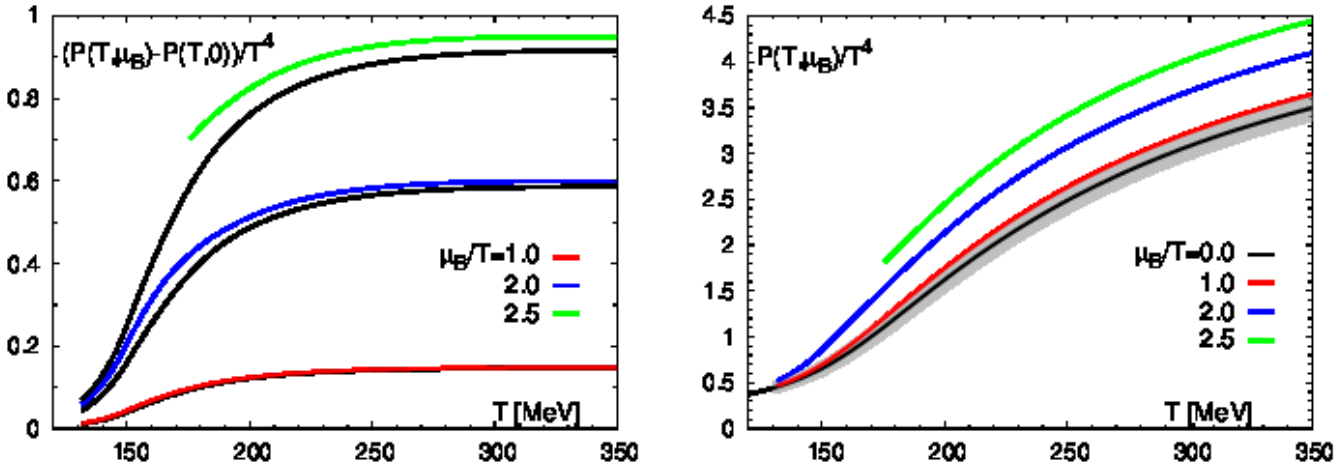

Figure: (Left) The μ_B-dependent part of the pressure at $\mathcal{O}((\mu_B/T)^2)$ (black) and $\mathcal{O}((\mu_B/T)^4)$ (colored) (Hegde 2014). The latter is shown only in the temperature regime where the neglected corrections at $\mathcal{O}((\mu_B/T)^6)$ contribute less than 10%. (Right) Combined with the $\mu_B = 0$ contribution to the pressure the neglected terms contribute less than 3% (Hegde 2014). The grey band shows the uncertainty of the black curve, which is a parametrization for $\mu = 0$ (Bazavov 2014).

EoS : The μ-dependent part of the pressure

Newest status : see C. Schmidt at "Extreme QCD", Plymouth, UK, August 2016:

`https://conference.ippp.dur.ac.uk/event/530/sessi`

Outline

Imaginary chemical potential $\mu = i\mu_I$ shifts the pseudocritical β_c oppositely to real μ

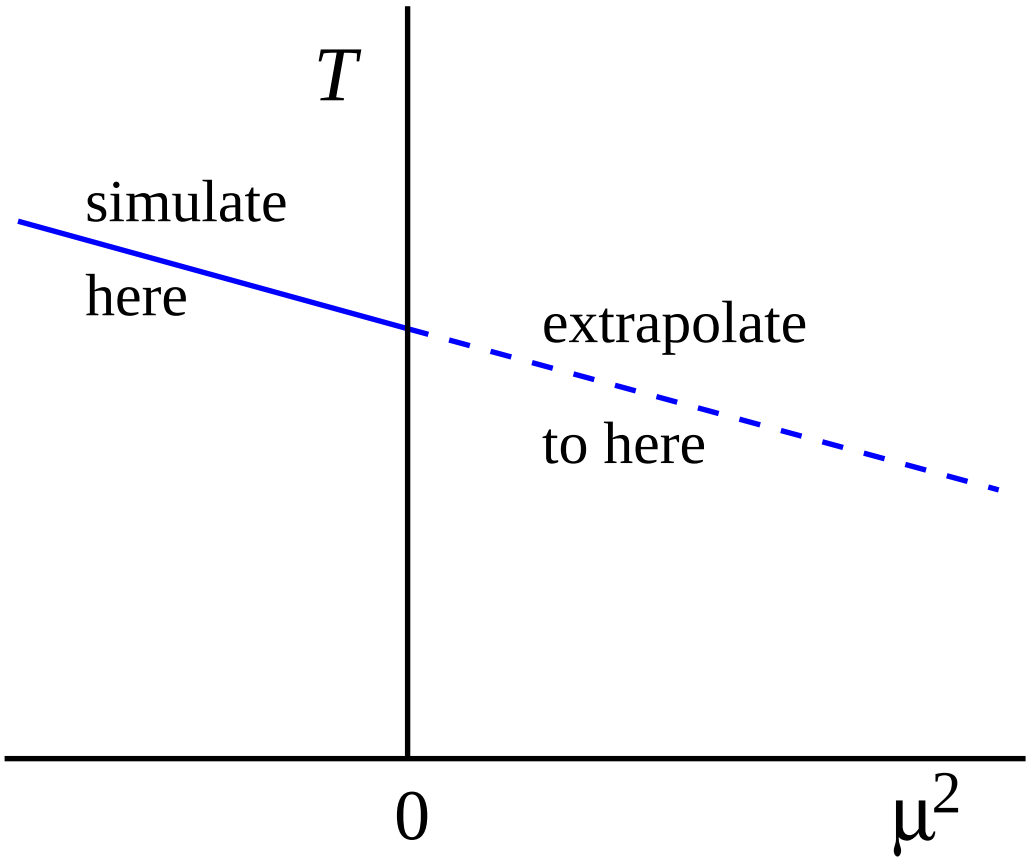

Figure: Phase boundary around $\mu^2 = 0$ in the (μ^2, T) plane.

Imaginary chemical potential does not only enable (again) standard updating, ...

... in fact, QCD at imaginary chemical potential is a much richer topic than one could have predicted. It has an intricate phase structure due to the following reasons:

- the interplay of chemical potential and center symmetry;
- the sensitivity of the thermal transition to the masses of the three light quarks (u, d, s).

One can discuss this, starting from the quark mass dependence of the thermal transition, summarised in the so-called "Columbia plot".
One can discuss center symmetry in pure SU(3) gauge theory and with the addition of quarks, and finally extend the "Columbia plot" to three dimensions $(m_{u,d}, m_s, \mu_{u,d})$, with light chemical potential $\mu_{u,d}$.

The Columbia plot for two light and one heavier quark species

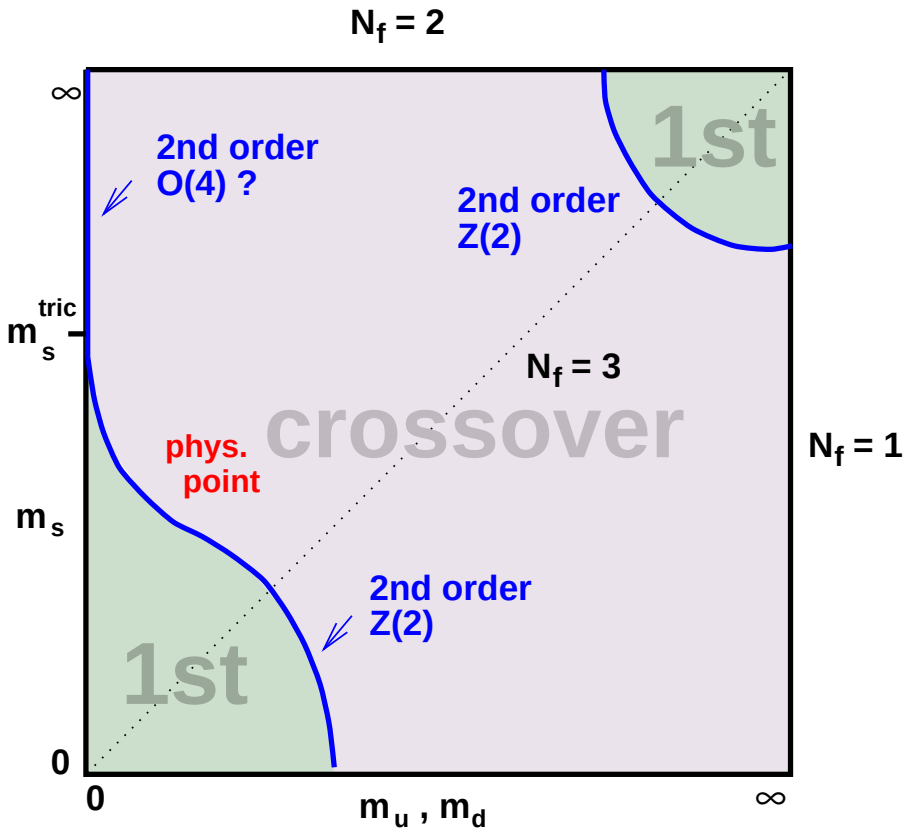

Figure: The "Columbia plot" is localizing, in a quark mass plot, where the phase transition is of first order, of second order and where it is a crossover (namely in most of the plot).

Analytical continuation of the pseudo-critical temperature

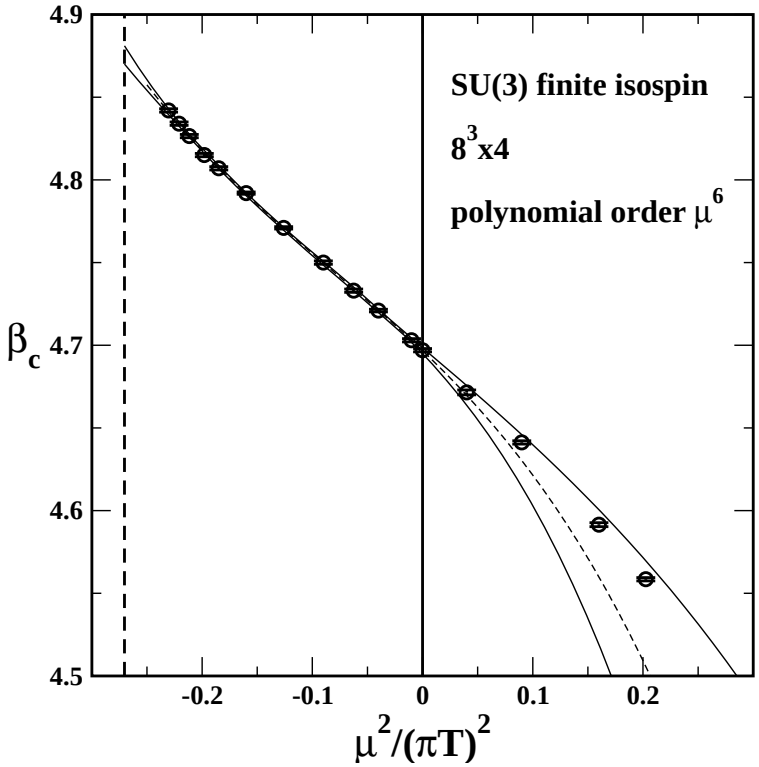

Figure: Analytic continuation of the pseudo-critical line $T_c(\mu)$ from $\mu^2 < 0$ to $\mu^2 > 0$: for imaginary μ the Taylor series is alternating, making the precise determination of the subleading Taylor coefficients and the continuation difficult (Cea 2009).

Roberge-Weiss transition

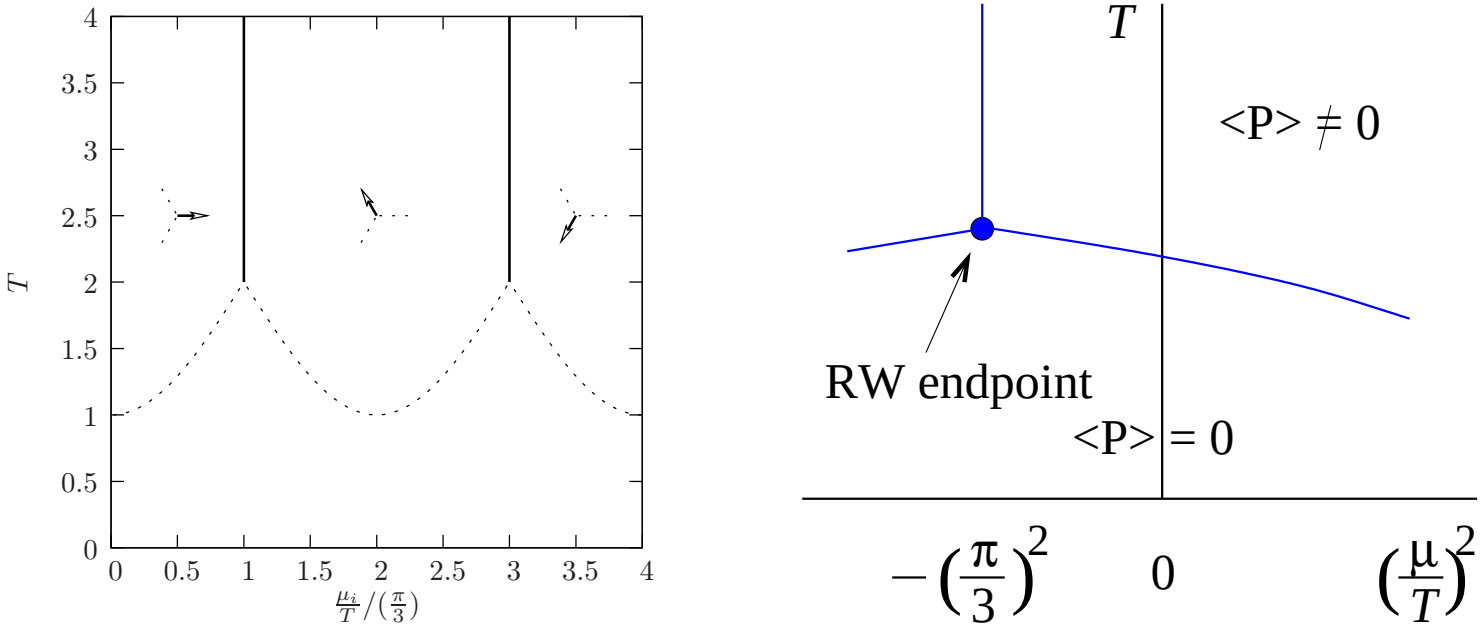

Figure: Phase structure in the (μ_I, T) plane (de Forcrand 2010) (left) and the (μ^2, T) plane (right). The vertical lines (left) and the vertical line entering the RW end point (righT) are first order transitions. The arrows show the complex orientation of the non-vanishing Polyakov loop throughout the three $Z(3)$ high-temperature sectors.

Modified Columbia plot at imaginary chemical potential

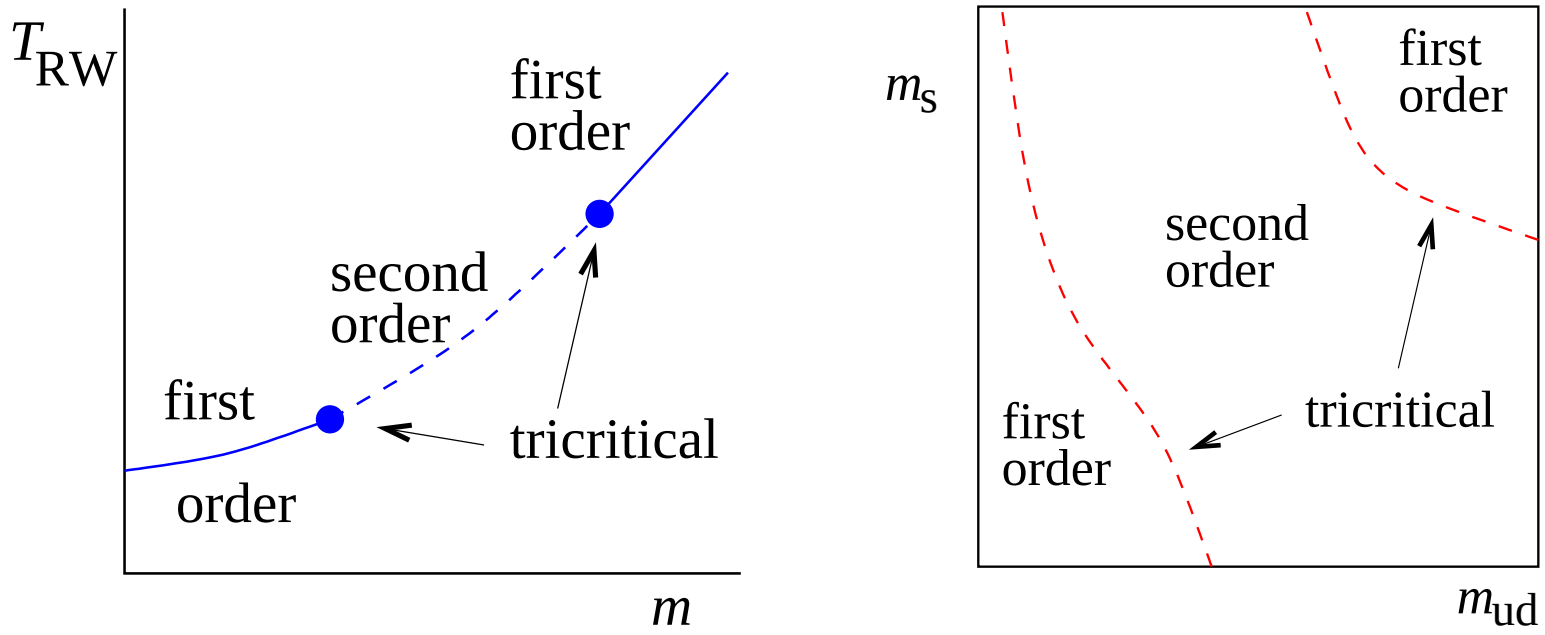

Figure: Left: Quark mass dependence of the temperature of the Roberge-Weiss endpoint, $T_{\rm RW}$, for $N_f = 3$: the first order "corners" grow. Right: equivalent of the "Columbia plot" at $\mu_{\rm I} = (\pi/3)T$. It is possible to obtain the curvature of the second-order transition surface on the real-μ side.

Extension of the Columbia plot to $\mu \neq 0$

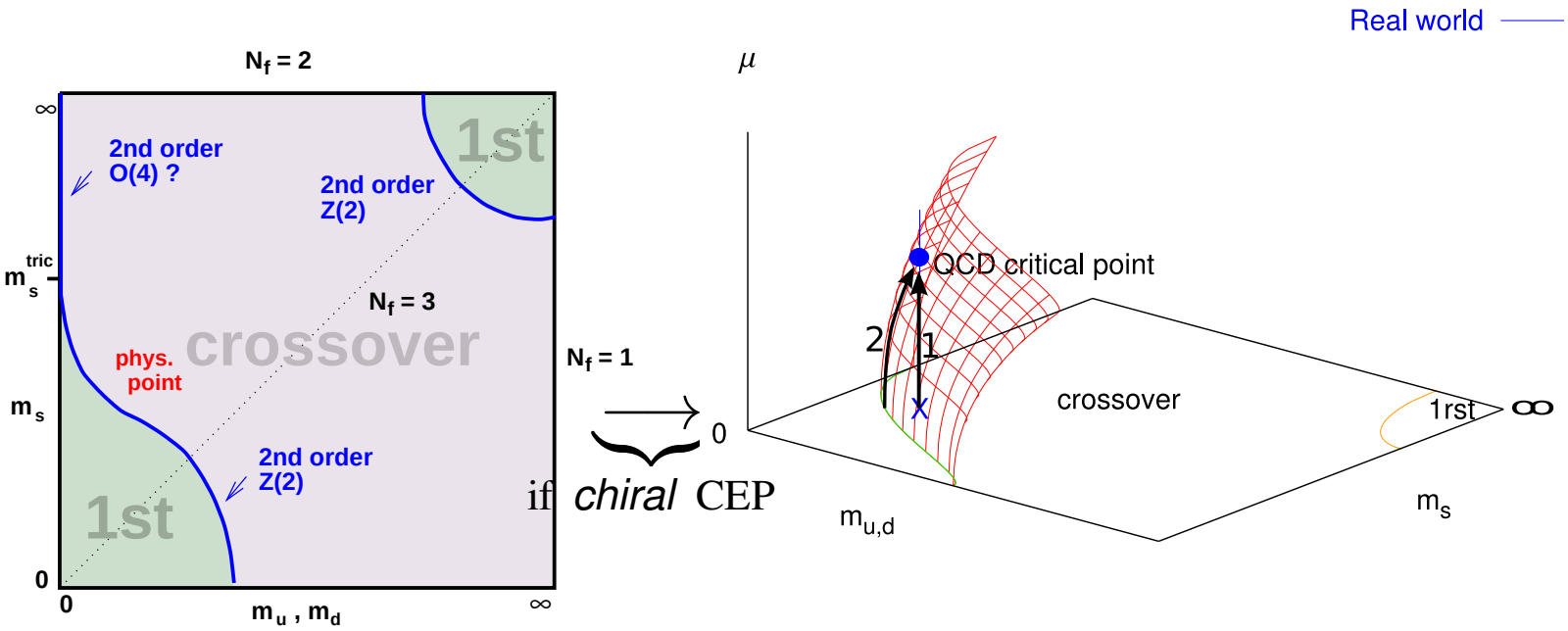

Figure: (*Left*) Order of the $\mu = 0$ finite temperature transition as a function of the light and strange quark masses ("Columbia plot"). (*Right*) Two ways to approach the chiral critical point : (1) at fixed physical quark masses or (2) along the critical surface climbing up from the 2nd order critical line in the $\mu = 0$ plane.

Possible scenarios: does the CEP exist, not exist or reappear at higher μ ?

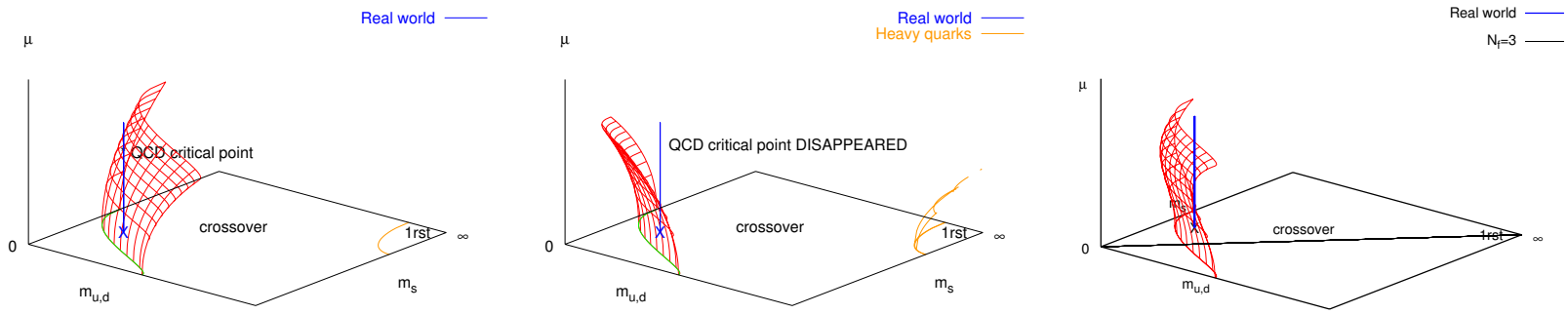

Figure: Possible scenarios for the curvature of the second-order surface for light quarks and the critical endpoint for physical quark masses (deForcrand 2010). (*Left*) critical endpoint exists at non-zero μ in case of outward curvature ; (*Center*) critical endpoint does not exist at non-zero μ in case of inward curvature ; (*Right*) **a more complicated second-order surface may lead to a reappearing critical endpoint.**

Outline

Another type of simulation ?

- Straightforward importance sampling combined with or without reweighting is typically not viable in a uniform manner, i.e. uniformly in the $\mu - T$ plane.
- At small μ/T it might be feasible to preserve the overlap as best as possible, on small volumes, or to use approximate methods, such as a Taylor series expansion or analytical continuation and scaling from imaginary chemical potential.
- To fully attack the sign problem, however, something more radical is needed and the configuration space, usually of $SU(3)$ matrices, should be
  1. redefined, picking variables dual to the links in the action ("dualization") or
  2. explored in a different manner, which might require a slight (controllable ?) extension ("complexification").

Another kind of configuration space ?

Given the excessive cancelation between configurations with "positive" and "negative" weight, one may wonder whether it is possible to give a sensible meaning to the concept of "dominant configurations" ? One should be prepared, if necessary, to accept instead an extended configuration space, as illustrated in next Figure:

- from real-valued degrees of freedom to generically complex ones
- from $SU(N)$ valued link matrices to more general ones: $SL(N, \mathbb{C})$.

Keep in mind: finally only the weighted averages make sense physically (as quantum averages) !

Simplifying the complex measure by going to complex variables

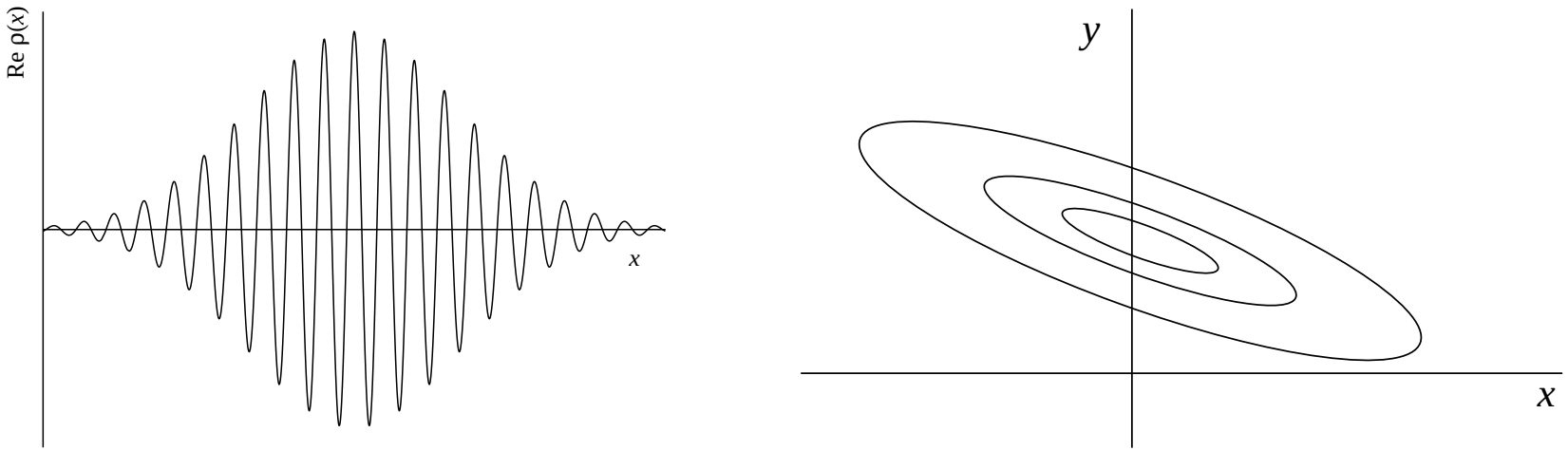

Figure: What are the dominant configurations in a path integral with a complex weight? All x seem of equal importance ! In complex Langevin dynamics, the question is answered by extending the configuration space into the complex plane (with a positive definite distribution $P(x, y)$ which is defined only there).

Simplifying the complex measure by going to complex variables

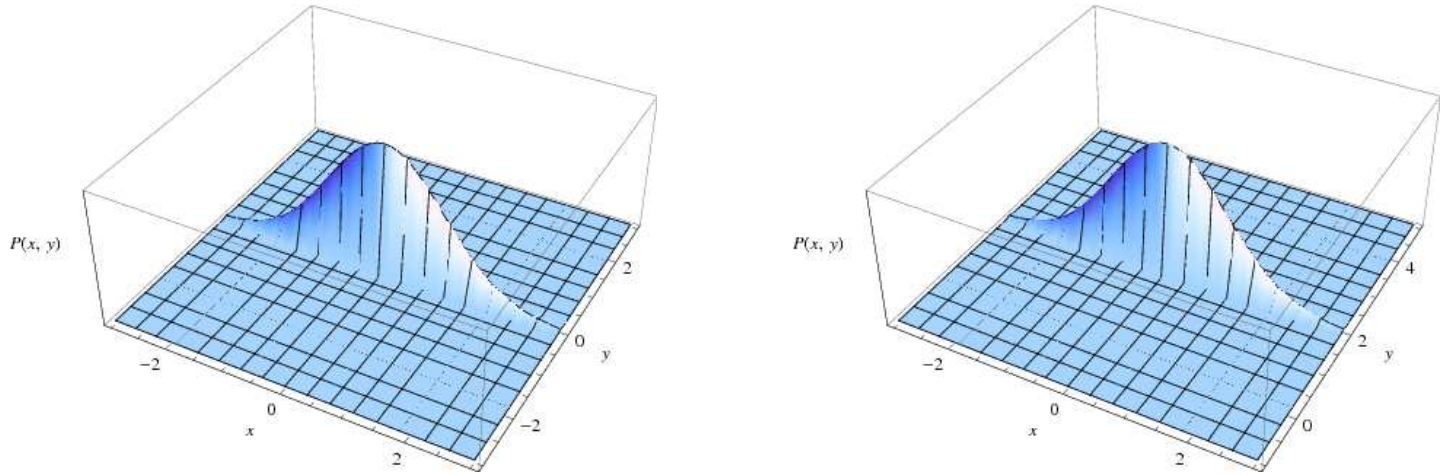

Figure: Distribution $P(x, y)$ for the action $S = \frac{1}{2}ax^2 + ibx$, for $a = 1$ and $b = 0$ (left), $b = -2$ (right).

Steps towards the Langevin dynamics, that we actually need

Real Langevin dynamics (real variable x, real action)

Real action $S(x)$ defines the measure to simulate:

$$P_{\text{equilibrium}}(x) \propto \exp\left(-S(x)\right)$$

A substitute for Monte Carlo : the Langevin equation

$$\frac{\partial x(\tau)}{\partial \tau} = -\frac{\partial S(x)}{\partial x}|_{x(\tau)} + \eta(\tau) \qquad \text{(white noise)}$$

Ensemble view : a Fokker-Planck equation for $P(x,\tau)$

$$\frac{\partial P(x,\tau)}{\partial \tau} = \frac{\partial}{\partial x}\left[\frac{\partial}{\partial x} + \frac{\partial S(x)}{\partial x}\right] P(x,\tau).$$

This reveals : the long-time limit is of the wanted form:

$$\lim_{\tau\to\infty} P(x,\tau) = P_{\text{equilibrium}}(x).$$

Valid also for many degrees of freedom (real field theory).

Steps towards the Langevin dynamics that we actually need

Complex Langevin dynamics
(complex variable $x + iy$, complex action)
Complex action $S(z) = S(x + iy)$ defines the measure we have to simulate:

$$P_{\text{equilibrium}}(x, y) \propto \exp\left(-S(x + iy)\right)$$

A substitute for Monte Carlo : the Langevin equation

$$\frac{\partial x(\tau)}{\partial \tau} = -\text{Re}\frac{\partial S(z)}{\partial z}|_{z(\tau)=x(\tau)+iy(\tau)} + \eta(\tau) \text{ (real white noise)}$$

$$\frac{\partial y(\tau)}{\partial \tau} = -\text{Im}\frac{\partial S(z)}{\partial z}|_{z(\tau)=x(\tau)+iy(\tau)} \quad \text{(without noise !)}$$

Ensemble view : a Fokker-Planck equation for $P(x, y, \tau)$

$$\frac{\partial P(x, y, \tau)}{\partial \tau} = \frac{\partial}{\partial z}\left[\frac{\partial}{\partial z} + \text{Re}\frac{\partial S(z)}{\partial z} + \text{Im}\frac{\partial S(z)}{\partial z}\right] P(x, y, \tau).$$

What can be achieved by complex Langevin dynamics ?

The Fokker-Planck form of quantum averages shows that the long-time limit of $P(x, y, \tau)$ is of the wanted form:

$$\lim_{\tau\to\infty} \int dx\, dy\, P(x, y, \tau)\, O(x + iy) = \langle O(x + iy)\rangle|_{\text{equilibrium}}$$
$$= \langle O(x + iy)\rangle|_{\text{noise } \eta}.$$

$\langle \ldots \rangle|_{\text{equilibrium}}$ was not possible to obtain by Monte Carlo.

Instead, the noise-average $\langle \ldots \rangle|_{\text{noise } \eta}$ is what we are now able to obtain from complex Langevin simulations.
Valid also for many degrees of freedom (complex scalar field theory).
Thus, finally, stochastic quantization (1981 invented by G. Parisi and Y.-S. Wu) has been successfully extended to complex actions.

Conditions of validity of complex Langevin simulations

General conditions of validity:

- holomorphic action $S(z)$, as well as holomorphic drift term and holomorphic observables
- distribution $P(x, y) \to 0$ fast enough with $y \to \infty$

Then the complex Langevin method ...

- not only converges, but it
- converges to the correct result !

Open question: can meromorphic drift terms spoil this derivation ?
This is a topic of hot current research ! see Lattice 2016 (24-30 July 2016)

Successful applications

- solving the 4-dimensional charged Bose gas with non-zero chemical potential reproducing the Silver Blaze effect.
- solving effective 3-dimensional Polyakov spin models as substitute for finite-density QCD, formulated in terms of Abelian spins ($P(\vec{x}) \in Z(N)$) or non-Abelian spins ($P(\vec{x}) \in SU(3)$).
- helped to understand the differences between Abelian (wrong) and non-Abelian (successful) spin models.

Outline

Recent interest triggered by ....

... successful applications to SU(3) gauge theory,

- first, in the presence of heavy (static) quarks with a simplified fermionic action written in terms of Polyakov loops coupled to full gauge dynamics)
- after that, also in the presence of a fully dynamical light quark action.

In $SU(N)$ gauge theories, the complexification works as follows (Berges 2006, Aarts 2008):
Originally the gauge links $U_{x\nu}$ are elements of $SU(N)$, i.e., they are unitary with determinant equal to unity. After discretisation of the Langevin time (time step ϵ) and using a lowest-order scheme in ϵ, a usual Langevin update takes the form (Batrouni 1985, also used in NSPT)

$$\begin{aligned} U_{x\nu}(n+1) &= R_{x\nu}(n)\, U_{x\nu}(n), \\ R_{x\nu} &= \exp\left[i\lambda_a \left(\epsilon K_{x\nu a} + \sqrt{\epsilon}\eta_{x\nu a}\right)\right]. \end{aligned}$$

Further details of stochastic quantization for gauge theories

The λ_a are the Gell-Mann matrices (sum over the indices $a = 1, \ldots N^2 - 1$). $K_{x\nu a}$ is the drift,

$$K_{x\nu a} = -D_{x\nu a}(S_{\rm YM} + S_{\rm F}), \quad S_{\rm F} = -\ln\det M,$$

including the logarithm of the fermion determinant.
Differentiation is defined as left Lie derivative :

$$D_{x\nu a} f(U) = \frac{\partial}{\partial\alpha} f\left(e^{i\alpha\lambda_a} U_{x\nu}\right)\Big|_{\alpha=0},$$

and the noise is normalised as usual,

$$\left\langle \eta_{x\nu a}(n)\eta_{x'\nu' a'}(n')\right\rangle = 2\delta_{xx'}\delta_{\nu\nu'}\delta_{aa'}\delta_{nn'}.$$

Since the Gell-Mann matrices are traceless, the determinant of R and hence of U remain equal to unity for any choice of K and η.

Rules of complexification

If the action and therefore the drift K are real, R and U will remain unitary, undergoing the Langevin update.
Consider now the case that the action (or the fermion determinant) is complex.
In that case $K^\dagger \neq K$ and U will no longer be unitary.
Instead, U will take values in the special linear group, i.e. complexification in this case is from $SU(N)$ to $SL(N,\mathbb{C})$.
$U^\dagger$ and U^{-1} are no longer identical.
Since complex Langevin dynamics provides the analytical continuation of the original theory, links have to be written as U or U^{-1}, respectively, (no more $U^\dagger$!) in the action.
Then $S(U)$ is a holomorphic function of U in principle (ignoring possible problems due to the fermion determinant here).

Keeping complexification under control

The original statement of unitarity, $UU^\dagger = \mathbb{1}$, is now replaced with the trivialiy $UU^{-1} = \mathbb{1}$, which, of course, holds and defines U^{-1}.

Physical observables should also be written as functions of U and U^{-1}, such that they are holomorphic, too.

On the other hand, nonholomorphic combinations can be used to monitor the complex Langevin process while it is "cruising" far away from the $SU(3)$ submanifold.

The deviation of links U from the $SU(N)$ manifold can be expressed by the so-called unitarity norms

$$d_1 = \frac{1}{N\,V_4} \sum_{x,\nu} \mathrm{Tr}\,\left(U_{x,\nu} U^\dagger_{x,\nu} - \mathbb{1} \right) \geq 0,$$

$$d_2 = \frac{1}{N\,V_4} \sum_{x,\nu} \mathrm{Tr}\,\left(U_{x,\nu} U^\dagger_{x,\nu} - \mathbb{1} \right)^2 \geq 0.$$

Deviations of the links from unitarity

Indeed, during a complex Langevin simulation these norms stray away from zero as demonstrated in the next Figure for a heavy-dense QCD simulation for two values of the chemical potential μ.

The heavy-dense effective theory

gauge action of Wilson type

$$S_{\text{gauge}} = -\frac{\beta}{6}\sum_{x}\sum_{\mu<\nu}\text{Tr}\,\left[U_{x,\mu\nu}+U^{-1}_{x,\mu<\nu}\right]$$

The fermion determinant being approximated by

$$\det M = \prod_{N_f}\prod_{\vec{x}}\det\left[1+he^{+\mu/T}\mathcal{P}_{\vec{x}}\right]^2\det\left[1+he^{-\mu/T}\mathcal{P}^{-1}_{\vec{x}}\right]^2$$

in terms of (inverse) Polyakov loops which are coupled to the pure gauge theory.

The Polyakov loop is written as usual

$$\mathcal{P}_{\vec{x}} = \prod_{\tau=0}^{N_\tau-1} U_{\vec{x},\tau,4},$$

the inverse Polyakov loop is written in terms of U^{-1}

$$\tau=0$$

The parameters of HDET are :

- inverse gauge coupling β (regulating the temperature)
- density parameter (from hopping parameter κ expansion)

$$z = h\, e^{\mu/T} = (2\kappa e^{\mu})^{N_\tau}$$

Deviation from $SU(3)$-valuedness in the course of complex simulation

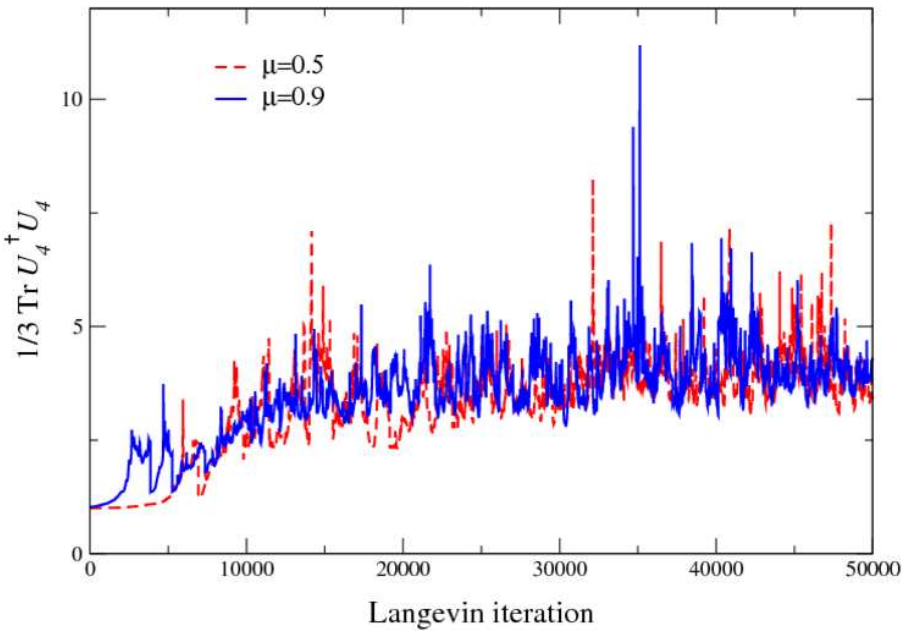

Figure: Deviation from $SU(3)$: Langevin time evolution of the unitarity norm $\mathrm{Tr}\, U_4^\dagger U_4/3 \geq 1$ in heavy dense QCD on a 4^4 lattice with $\beta = 5.6$, $\kappa = 0.12$, $N_f = 3$ (from Aarts 2008).

Gauge cooling drives towards the unitary submanifold

Intuition tells us that during a simulation the evolution should be controlled in the following way: configurations should stay close to the $SU(N)$ submanifold

- when the chemical potential μ is small;
- with small non-unitary initial conditions;
- as a result of roundoff errors.

In practice however, the unitary submanifold turns out to be unstable. This has been observed many times.
The relation between this and the breakdown of the approach – convergence to incorrect results – has recently been understood.
Gauge cooling will really save the complex Langevin process from ending in run-away "trajectories".

The instability results from the gauge freedom

The instability of the $SU(N)$ submanifold is related to gauge freedom. Consider a link at site x, which transforms as

$$U_{x,nu} \to \Omega_x U_{x,\nu} \Omega^{-1}_{x+\hat{\nu}}, \qquad \Omega_x = e^{i\omega^a_x \lambda_a},$$

with ω^a_x being the gauge parameters.
In $SU(N)$, gauge parameters $\omega^a_x \in \mathbb{R}$, while in $SL(N,\mathbb{C})$, the gauge parameters $\omega^a_x \in \mathbb{C}$.
While unitary gauge transformations preserve the unitarity norms, $SL(N,\mathbb{C})$ transformations with ω^a_x being non-real, do not.
In principle, those transformations can make the unitarity norms increase beyond any bounds, resulting in broad undesirable distributions.
Having made this observation, one can use it in a constructive way.

A gauge relaxation choice : gauge cooling

It is possible to devise gauge transformations that can systematically reduce the unitarity norms (of the links around) and hence control the Langevin evolution.
This is called gauge cooling (Seiler/Sexty 2012).
We consider the effect of a gauge trafo localized at x,

$$U_{x,\nu} \to \Omega_x U_{x,\nu}, \qquad U_{x-\hat{\nu},\nu} \to U_{x-\hat{\nu},\nu}\Omega_x^{-1}, \qquad \Omega_x = e^{-\alpha f_x^a \lambda_a},$$

with $\alpha > 0$, i.e. a cooling update acting at site x.
What is the effect of this on the total unitarity norm d_1 ?
After one update and linearising in α, we find

$$d_1' - d_1 = -\frac{\alpha}{N}(f_x^a)^2 + \mathcal{O}(\alpha^2) < 0,$$

in other words, in linear order the average distance from $SU(N)$ has indeed been reduced.

A clever choice for gauge relaxation : gauge cooling derived from the unitarity norm itself

So far, f_x^a was not defined. One may chose it as the gradient of the unitarity norm itself,

$$f_x^a = 2\mathrm{Tr} \sum_\nu \left[\lambda_a \left(U_{x,\nu} U_{x,\nu}^\dagger - U_{x-\hat{\nu},\nu}^\dagger U_{x-\hat{\nu},\nu} \right) \right]$$

When all $U \in SU(N)$ we get $f_x^a = 0$, and cooling has no effect at all.
Otherwise, the distance to the $SU(n)$ submanifold is systematically reduced iteratively.
In a multilink model, the total distance decreases not exponentially but powerlike.

The real recipe

In the actual complex Langevin update, Langevin updates and gauge cooling steps are applied in alternating order (eventually more cooling steps per Langevin step).

As long as the "stochastic gauge fixing" runs, the link matrices U are not on the unitarity surface.

Is this a problem ?

In normal gauge fixing one can hope to "gauge-fix" every Monte Carlo or Hybrid Monte Carlo configuration (which represents an "orbit") to the desired gauge (Landau, Coulomb etc.).
The problem is there: Gribov ambiguity, i.e. non-uniqueness of the gauged copy.

Can a gauge configuration (finally ?) be reduced to $SU(3)$? (analog to gauge fixing)

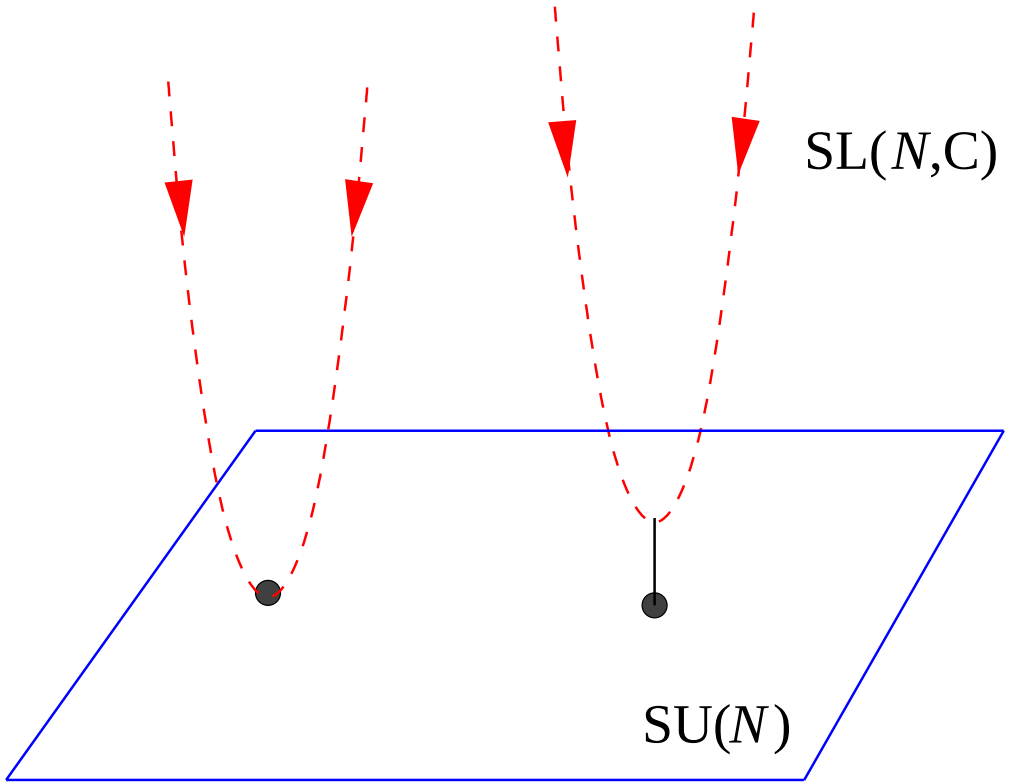

Figure: Gauge cooling of links in $SL(N,\mathbb{C})$ reduces the distance from $SU(N)$. The left orbit is equivalent to a $SU(N)$ configuration, while the one on the right is not (Aarts 2013).

Outline

Trying to avoid the sign problem by using the canonical approach

Simulations at imaginary chemical potential, obtain $Z_{GC}(\mu = i\mu_I)$. Then get the microcanonical partition function via Fourier transformation:

$$\begin{aligned} Z_C(T,n) &= \frac{1}{2\pi}\int_{-\pi}^{\pi} d\left(\frac{\mu_I}{T}\right) e^{-in\mu_I/T} Z_{GC}(T,\mu = i\mu_I) \\ &= \frac{3}{2\pi}\int_{-\pi/3}^{\pi/3} d\left(\frac{\mu_I}{T}\right) e^{-in\mu_I/T} Z_{GC}(T,\mu = i\mu_I) \end{aligned}$$

RW-periodicity in μ_I : $Z_{GC}(\mu_I/T) = Z_{GC}(\mu/T + 2\pi/3)$
this implies $\rightarrow$ only integer baryon numbers $B = n/3$ ($n = 0$ *mod* 3) are allowed.
The integral can be restricted to the interval $[-\pi/3, \pi/3]$ which is repeated by periodicity.

Problems of the canonical approach

- Fourier transformation of noisy data !
- Need a fine grid in μ_I !
- Need the result for large baryon numbers, in order to reproduce the grand-canonical results in the thermodynamic limit.
- Numerically very hard !
- Actually only small lattices so far !
- Extra high precision needed to perform the Fourier transformation over μ_I.

Canonical vs. Grand Canonical Ensemble, schematically

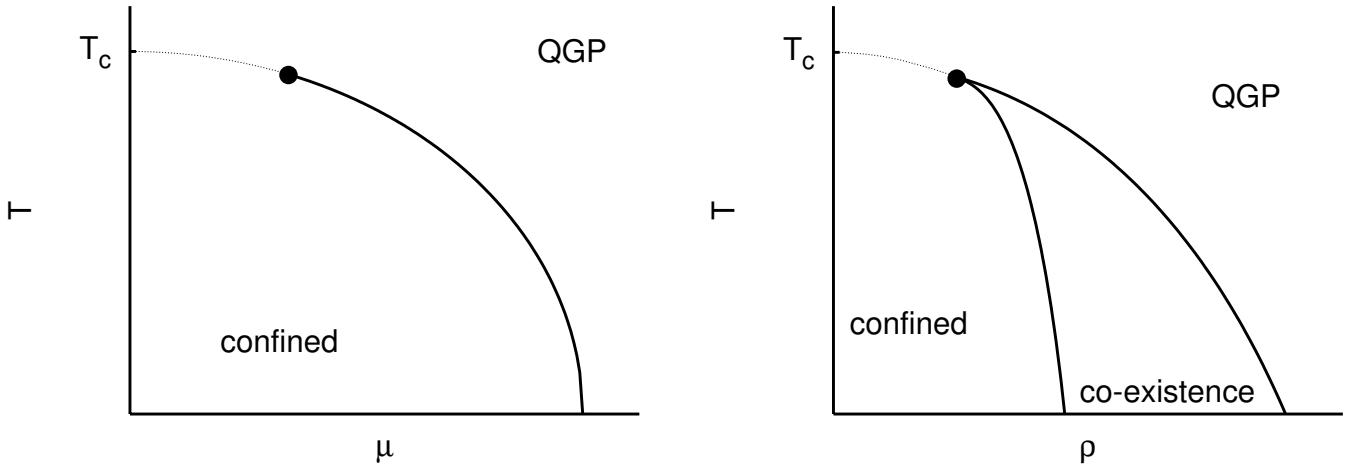

Figure: Sketch of the conjectured QCD phase diagram in the grand-canonical (T–μ plane) and canonical (T–ρ plane) formalism.

(from Kratochvila 2005)

Maxwell construction to find the phase boundaries

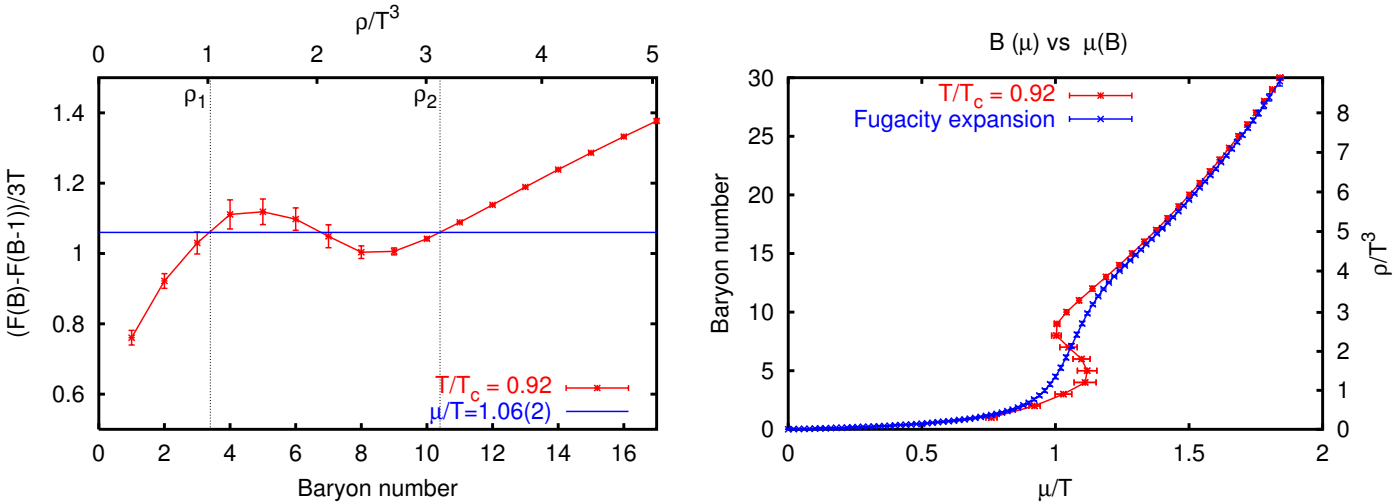

Figure: (left) The Maxwell construction allows to extract the critical chemical potential and the boundaries of the co-existence region. (right) Comparing the saddle point approximation (red) with the fugacity expansion (blue). Strong finite-size effects in the latter obscure the first-order transition.

(from Kratochvila 2005)

The number of flavors matters: $N_f = 4$ vs. $N_f = 2$

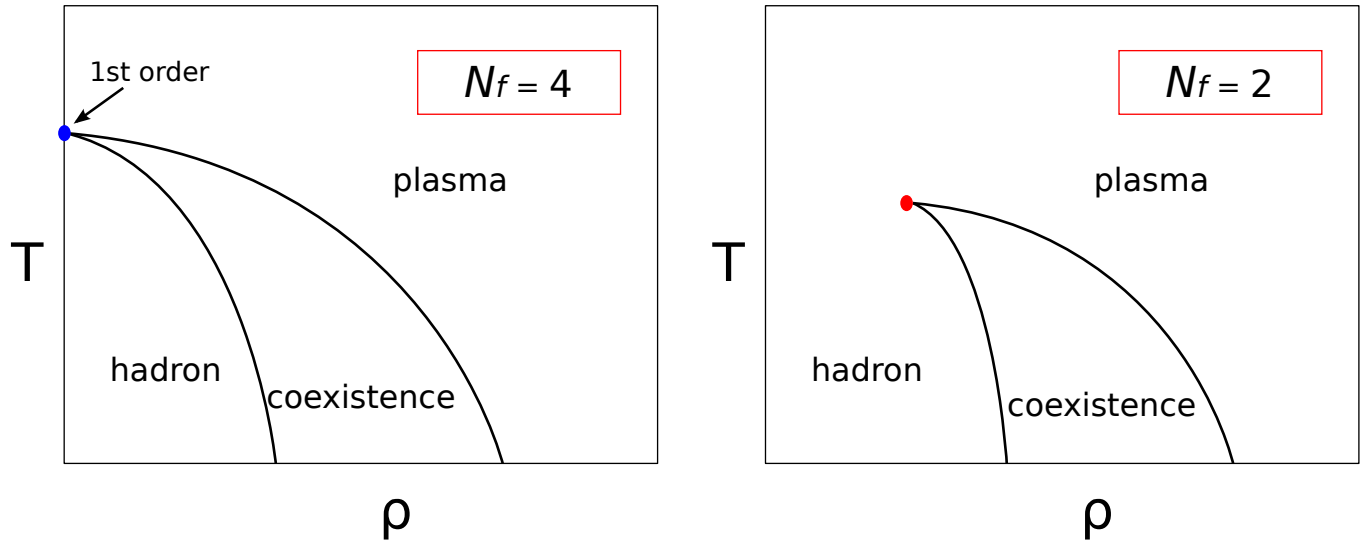

Figure: Schematic phase diagram of four and two flavors (i.e. light degenerate quarks) in the canonical ensemble. In the $N_f = 4$ case the endpoint at $\rho = 0$ is a first order thermal transition.

Trying to cure the sign problem by more radical measures to do grand canonical simulations

- Changing the order of integration, roughly speaking : do gauge field integration first, quark integration next
- Dual formulations (change the configuration space)
- Density of states, histogram methods
- Lefschetz thimbles

One example: The dual formulation

... trades the original configurations space for the expansion powers of a strong coupling expansion (High Temperature Expansion) of the partition function.
The remaining integrals in the configuration space often can be done beforehand and result in constraints between the remaining variables, the (integer-valued) powers of the HTE (so-called "fluxes").
These constraints (mainly Kronecker deltas) hide (or better: take into account !) the sign problem: all cancellations are happening here !
Exploration of the new discrete "configuration space" by geometrical (worm, snake) algorithms which express (allow to handle) the constraints.
There is no field interpretation for a single "configuration".
Certain estimators for observables can be formulated, however.

One example : $SU(3)$ spin model for finite density QCD

The action of the $SU(3)$ spin model on a 3-d lattice is

$$S[L] = -\sum_x \left(\tau \sum_{\nu=1}^{3} \left[P(x)P(x+\hat{\nu})^\star + c.c. \right] \right) + \sum_x \kappa \left[e^{\mu} P(x) + e^{-\mu} P(x)^\star \right]$$

Degrees of freedom : $P(x) \in \mathbb{C}$ (spins $=$ Polyakov loops),

$$P(x) = \mathrm{Tr}\, L(x) \quad \text{with} \quad L(x) \in SU(3).$$

Partition function (defines the measure !) :

$$Z = \int_{SU(3)} \prod_x dL(x) e^{-S[L]}.$$

$dL(x)$ is the Haar measure (or reduced Haar measure).

The $SU(3)$ spin model for finite density QCD

Without "magnetic field term", i.e., for $\kappa = 0$, the system has a low temperature (or low τ) phase where $\langle P \rangle$ with $P = \frac{1}{V} \sum_x P(x)$ vanishes.

This corresponds to the confined phase.

At $\tau_c \sim 0.137$ the system undergoes a first order deconfinement transition between "confinement" and "deconfinement".

For small κ (high quark mass represented as "magnetic field") and $\mu = 0$ (zero density) the first order line persists ending in a second order endpoint (Wyld/Karsch 1985).

The dualization method shows that for $\mu > 0$ (at finite density, imbalance between P and $P^\star$) the first order transition is weakened further, i.e., the endpoint shifts towards smaller κ.

The $SU(3)$ spin model for finite density QCD

see: Y.D. Mercado and C. Gattringer, arXiv:1204.6074
Applying HTE techniques, the partition function can be rewritten in terms of new degrees of freedom, the flux variables.

$$Z = \sum_{\{l,\bar{l}\}} \sum_{\{s,\bar{s}\}} \left(\prod_{\overline{x},\nu} \frac{\tau^{l_{x,\nu}+\bar{l}_{x,\nu}}}{l_{x,\nu}!\ \bar{l}_{x,\nu}!} \right) \left(\prod_{x} \frac{\eta^{s_x}\ \overline{\eta}^{\bar{s}_x}}{s_x!\ \bar{s}_x!} \right) \left(\prod_{x} I(f_x, \bar{f}_x) \right)$$

τ is a monotonous function of the temperature, the other variables are

$$\eta = \kappa e^{\mu} \quad \text{and} \quad \overline{\eta} = \kappa e^{-\mu}$$

$$I(n,\overline{n}) = \int_{SU(3)} dL\, (\mathrm{Tr}L)^n\, (\mathrm{Tr}L^{\dagger})^{\overline{n}}$$

The $SU(3)$ spin model for finite density QCD

$I(n,\overline{n}) \neq 0$ only, if the triality condition $(n-\overline{n}) \bmod 3 = 0$ is obeyed.

In the "flux representation" for the partition sum the arguments of the $I(.,.)$ are the summed fluxes f_x and $\overline{f}_x$ at the sites x of the lattice defined by

$$f_x = \sum_{\nu=1}^{3} [\, I_{x,\nu} + \bar{I}_{x-\hat{\nu},\nu} \,] + s_x \qquad \overline{f}_x = \sum_{\nu=1}^{3} [\, \bar{I}_{x,\nu} + I_{x-\hat{\nu},\nu} \,] + \overline{s}_x$$

The triality condition for non-vanishing weights $I(.,.)$ then reads more explicitly

$$(\, f_x - \overline{f}_x \,) \bmod 3 = 0 \,, \tag{6}$$

which introduces a constraint for the allowed values of the "dimer and monomer variables" meeting at a lattice site x.

Reparametrization

For the advantage of updates,
one choses new integer valued dimer variables
$k_{x,\nu} \in [0, +\infty)$ and $\overline{k}_{x,\nu} \in (-\infty, +\infty)$, which are related to the old dimer variables via $l_{x,\nu} - \bar{l}_{x,\nu} = \overline{k}_{x,\nu}$ and $l_{x,\nu} + \bar{l}_{x,\nu} = |\overline{k}_{x,\nu}| + 2k_{x,\nu}$.
Similarly one defines new integer valued monomer variables
$r_x \in [0, +\infty)$ and $\overline{r}_x \in (-\infty, +\infty)$ which are related to the old monomer variables via $s_x - \overline{s}_x = \overline{r}_x$ and $s_x + \overline{s}_x = |\overline{r}_x| + 2r_x$.

Estimators in terms of the flux variables

Defining the following abbreviations for the sums of dimer and monomer variables,

$$K \equiv \sum_{x,\nu} [|\overline{k}_{x+\nu}| + 2k_{x+\nu}]$$

$$R \equiv \sum_x r_x \ , \ \overline{R} \equiv \sum_x \overline{r}_x \ , \ |\overline{R}| \equiv \sum_x |\overline{r}_x|$$

flux representations for the internal energy U, the heat capacity C, the Polyakov loop expectation value $\langle P \rangle$, and the Polyakov loop susceptibility χ_P can be given

$$\begin{aligned} U &= \left\langle \, K + |\overline{R}| + 2R \, \right\rangle \\ C &= \left\langle \, \left[(K + |\overline{R}| + 2R) - U \right]^2 - (K + |\overline{R}| + 2R) \, \right\rangle \end{aligned}$$

Estimators in terms of flux variables

and

$$\langle P \rangle = \frac{1}{\eta} \left\langle \frac{|\overline{R}| + \overline{R}}{2} + R \right\rangle$$

$$\chi_P = \left\langle \left[\frac{1}{\eta} \left(\frac{|\overline{R}| + \overline{R}}{2} + R \right) - \langle P \rangle \right]^2 - \frac{1}{\eta^2} \left(\frac{|\overline{R}| + \overline{R}}{2} + R \right) \right.$$

Qualitative similarity to the phase diagram of QCD

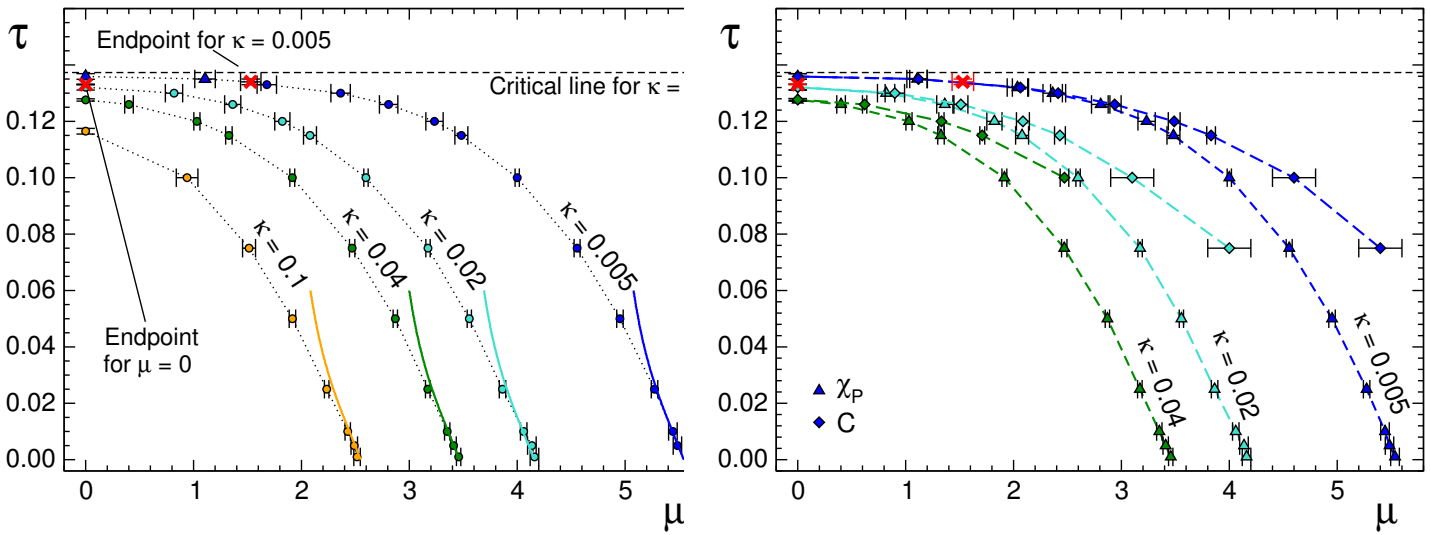

Figure: (left) The phase diagram as a function of τ and μ for different values of κ (inverse mass). The phase boundaries (symbols connected with dotted lines) were determined from the maxima of χ_P. (right) Comparison of the maxima of χ_P (triangles) and heat capacity C (diamonds).

(from Mercado/Gattringer 2012)

The dual formulation for ϕ^4 theory at finite density

see: C. Gattringer and Kloiber, arXiv:1206.2954

$$S = \sum_x \left(\eta |\phi_x|^2 + \lambda |\phi_x|^4 - \sum_{\nu=1}^{4} \left[e^{\mu\ \delta_{\nu,4}} \phi_x^* \phi_{x+\widehat{\nu}} + e^{-\mu\ \delta_{\nu,4}} \phi_x^* \phi_{x-\widehat{\nu}} \right] \right)$$

From integrating $\int \prod_x d^2\phi_x \ \exp(-S)$ follows the constraint, that "current conservation"

$$\sum_\nu [n_{x,\nu} - \overline{n}_{x,\nu} - (n_{x-\widehat{\nu},\nu} - \overline{n}_{x-\widehat{\nu},\nu})] = 0$$

must be fulfilled in any point x.

The dual formulation reproduces the Silver Blaze effect

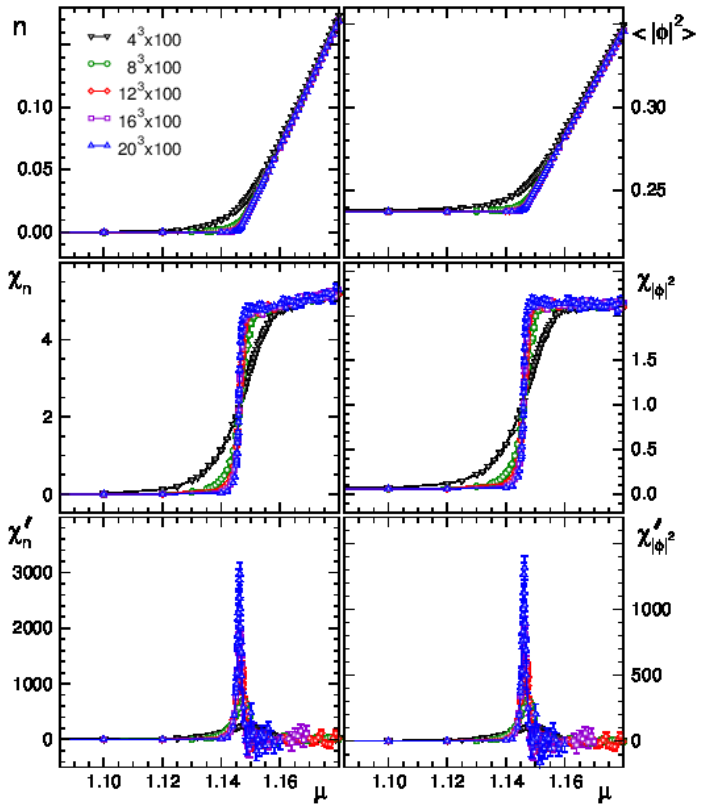

Figure: Results at $T = 0.01$ for $\eta = 9.0$ and $\lambda = 1.0$. In the lhs. column of plots we show n, χ_n and χ'_n as a function of μ (top to bottom). In the rhs. column we show $\langle|\phi|^2\rangle$, $\chi_{|\phi|^2}$ and $\chi'_{|\phi|^2}$.

Outline

Where all this has led us to ?

The attempts to seriously deal with field theory at finite baryonic density (θ angle etc.) have opened a rich field of interesting techniques not known/foreseen before.

I hope, that somebody of you got interested in this topic.

Thank you for your attention !

Recommended articles

- O. Philipsen "The QCD equation of state from the lattice", arXiv:1207.5999
  (Invited Review Article in "Progress in Particle and Nuclear Physics" March 2003))
  interesting for us : EoS for finite baryonic density, from Taylor expansion and imaginary μ
- O. Philipsen "Status of the QCD phase diagram from lattice calculations", arXiv:1111.5370
  (Lecture at HIC for FAIR workshop and XXVIII Max Born Symposium, Wroclaw, May 19-21, 2011)
- O. Philipsen "Lattice QCD at non-zero temperature and baryon density", arXiv:1009.4089
  (Lectures given at the Summer School on "Modern perspectives in lattice QCD", Les Houches, August 3-28, 2009)

Other recommendable article of general nature

- P. Petreczky (BNL)
  "Lattice QCD at non-zero temperature",
  J. Phys. G: Nucl. Part. Phys. 39 (2012) 093002;
  arXiv:1203.5320
- Most recent:
  Heng-Tong Ding (CCNU Wuhan), F. Karsch (BNL and Bielefeld U), S. Mukherjee (BNL)
  "Thermodynamics of Strong-Interaction Matter from Lattice QCD"
  Int. J. Mod. Phys. E24 (2015) no.10, 1530007,
  arXiv:1504.05274

Two recommendable articles concentrated on $\mu \neq 0$

- Ph. de Forcrand
  "Simulating QCD at finite density"
  arXiv:1005.0539 PoS (LAT2009) 010
  (Plenary talk at Lattice 2009)
  Still conceptually very useful !
- Most recent:
  G. Aarts
  "Introductory lectures on lattice QCD at nonzero baryon number",
  arXiv:1512.05145
  (Lectures at the XIII International Workshop on Hadron Physics, Brazil, March 2015)
  Valuable guide to the literature !

I also recommend : my lectures at a previous Helmholtz Summer School in Dubna "Dense Matter 12"

`theor.jinr.ru/~dm12/lectures/Ilgenfritz_1.pdf`

... dealing with the real thing : lattice QCD on the 4-dimensional lattice at $\mu \neq 0$

`theor.jinr.ru/~dm12/lectures/Ilgenfritz_2ext.pdf`

... dealing with lattice-based effecive models and heuristic effective models (like "flux tube models" a la Patel) which have been formulated *ad hoc* and have been around for some time, being studied on a 3-dimensional lattice

My earliest, premature encounters with high density LQCD took place in the 80-s

- "Dynamical Fermions At Nonzero Chemical Potential And Temperature: Mean Field Approach", E.-M. I., J. Kripfganz, Z. Phys. C29 (1985) 79-82
- "QCD Thermodynamics and Non-Zero Chemical Potential", E.-M. I., J. Kripfganz, in "Hadronic Matter under Extreme Conditions", Kiev, 1986, part 1, p. 153
  Proceedings of a workshop organized in BITP Kiev by Gennady Zinovjev (that could not take place because of the Chernobyl desaster)
- "Complex Langevin Simulation Of Chiral Symmetry Restoration At Finite Baryonic Density", E.-M. I., Phys. Lett. B181 (1986) 327